Topical Review: Flash Sintering of Ceramic Materials

C. E. J. Dancer

International Institute for Nanocomposite Manufacturing, Warwick Manufacturing Group, University of Warwick, Coventry, CV4 7AL, United Kingdom

Abstract

During flash sintering, ceramic materials can sinter to high density in a matter of seconds while subjected to electric field and elevated temperature. This process, which occurs at lower furnace temperatures and in shorter times than both conventional ceramic sintering and field-assisted methods such as spark plasma sintering, has the potential to radically reduce the power consumption required for the densification of ceramic materials. This paper reviews the experimental work on flash sintering methods carried out to date, and compares the properties of the materials obtained to those produced by conventional sintering. The flash sintering process is described for oxides of zirconium, yttrium, aluminium, tin, zinc, and titanium; silicon and boron carbide, zirconium diboride, materials for solid oxide fuel applications, ferroelectric materials, and composite materials. While experimental observations have been made on a wide range of materials, understanding of the underlying mechanisms responsible for the onset and latter stages of flash sintering is still elusive. Elements of the proposed theories to explain the observed behaviour include extensive Joule heating throughout the material causing thermal runaway, arrested by the current limitation in the power supply, and the formation of defect avalanches which rapidly and dramatically increase the sample conductivity. Undoubtedly, the flash sintering process is affected by the electric field strength, furnace temperature and current density limit, but also by microstructural features such as the presence of second phase particles or dopants and the particle size in the starting material. While further experimental work and modelling is still required to attain a full understanding capable of predicting the success of the flash sintering process in different materials, the technique nonetheless holds great potential for exceptional control of the ceramic sintering process.

Keywords

Ceramics; flash sintering; sintering; densification; ceramic processing

Contents

1. Introduction

Conventional ceramic processing involves long, high temperature heat-treatments to consolidate and densify the material and form a mechanically robust polycrystalline structure. Without very carefully

designed process control, the high temperatures required for high levels of densification lead to significant grain growth from the starting particle size [1], making it difficult to maintain a nano-sized grain structure even where nanocrystalline starting materials are used [2]. Such high temperatures also limit the materials which can be co-processed with the ceramic to those with melting points above the sintering temperature. While alternatives to conventional ceramic sintering including pressure-assisted processes (hot isostatic pressing, spark plasma sintering, hot pressing) and microwave-mediated heating can reduce the temperatures required for sintering to full density, these generally require specialised equipment, have high power consumption, and, particularly in the case of pressure-assisted methods, significantly limit the geometry of the samples produced [3].

Flash sintering is an alternative sintering technology which was first developed by Rishi Raj of University of Colorado Boulder in 2010 [4]. Initially demonstrated for 8-mol% yttria-stabilised cubic zirconia (8YSZ), flash sintering involves a high electric field being passed through a specimen with simultaneous furnace heating. The observation of the phenomenon developed methods used in earlier work using lower electric fields for the suppression of grain growth [5–7]. An electric field is generated in the sample which decreases as the sample shrinks by sintering. The “flash” refers to the power surge observed during the process which sees sintering completed in a few seconds [8] at reduced furnace temperatures compared to conventional sintering. Flash sintering can result in significantly less grain growth compared to conventional sintering methods [9]. The ready production of nanostructured ceramic materials gives materials higher strength and toughness compared to the micron-scale equivalents [9]. Flash sintering therefore represents not only a route to more rapid manufacturing, but also to novel materials with fine nanostructured features. For this reason there has already been commercial interest in this area, with the UK-based company Lucideon leading developments in industrial versions of flash sintering [10].

This review summarises the work carried out in developing the flash sintering process for ceramic materials since the original observation of this phenomenon by Cologna *et al.* in 2010 [4]. Following a brief introduction to ceramic sintering terminology and processes, the flash sintering technique will be described in detail, identifying the important processing parameters and limitations which have

been observed to date. The ceramic materials which have already been shown to undergo flash sintering will be described in detail, and theories which aim to explain the underlying material mechanisms involved in the flash sintering process will be described. Finally, a summary of key processing variables will be presented, along with some indicative ideas for future work in this area.

2. Densification of ceramic materials by sintering

Ceramic materials have extremely high melting points in their pure forms and in consequence ceramic materials are typically consolidated to near net-shape dimensions by powder-processing and sintering at high temperatures [3]. The sintering process bonds the ceramic particles together into one contiguous body, strengthening the ceramic material and enhancing electrical properties through greater connectivity. Widespread discussion of the sintering process can be found in numerous textbooks and articles in the literature [1,3,11,12]; to aid the later discussion of the differences between conventional and flash sintering a brief description of the sintering process is given below.

2.1 Ceramic processing

A typical conventional sintering route to produce a ceramic disc is shown in Figure 1. Assuming the starting material is of the required composition, it can either be used as supplied by the manufacturer, or processed to incorporate additives such as binders, dispersants, or sintering aids, and/or to break up agglomerates. The milling/mixing process can be carried out with dry powders but is usually more efficient if water or an alcohol is used. After milling the powders are dried and usually passed through a sieve. This powder is then pressed in a mould of the required shape and compacted using uniaxial or cold-isostatic pressing. The pressed ceramic, known as a green compact before heat-treatment, is then fired in a furnace using a suitable heating cycle including a high temperature hold period which often lasts for an hour or more even in lab-scale equipment to allow thermal equilibrium and for densification mechanisms to operate across the entire sample. Where additives have been included the heating programme includes a low temperature isothermal hold stage in order to burn out the organic binder and dispersant. Heat treatments can be carried out in air, vacuum, or gaseous atmosphere,

depending on the material. In conventional ceramic processing the sample is freestanding during the process and is not placed under applied uniaxial or isostatic pressure. Once the sample has cooled to room temperature, it is removed for further shaping or polishing, characterisation, or direct use in the intended application. There are variations on this overall route at each stage; steps can be omitted, methods such as extrusion, 3D printing, or slip casting can be used to shape the samples, and heat treatments can vary considerably, including fast firing [13] where samples are only inserted into the hot zone of the furnace at high temperature, and are removed for rapid cooling. However, overall some version of the process described here and pictured in Figure 1 is used to produce the vast majority of ceramic samples which are made by solid-state sintering.

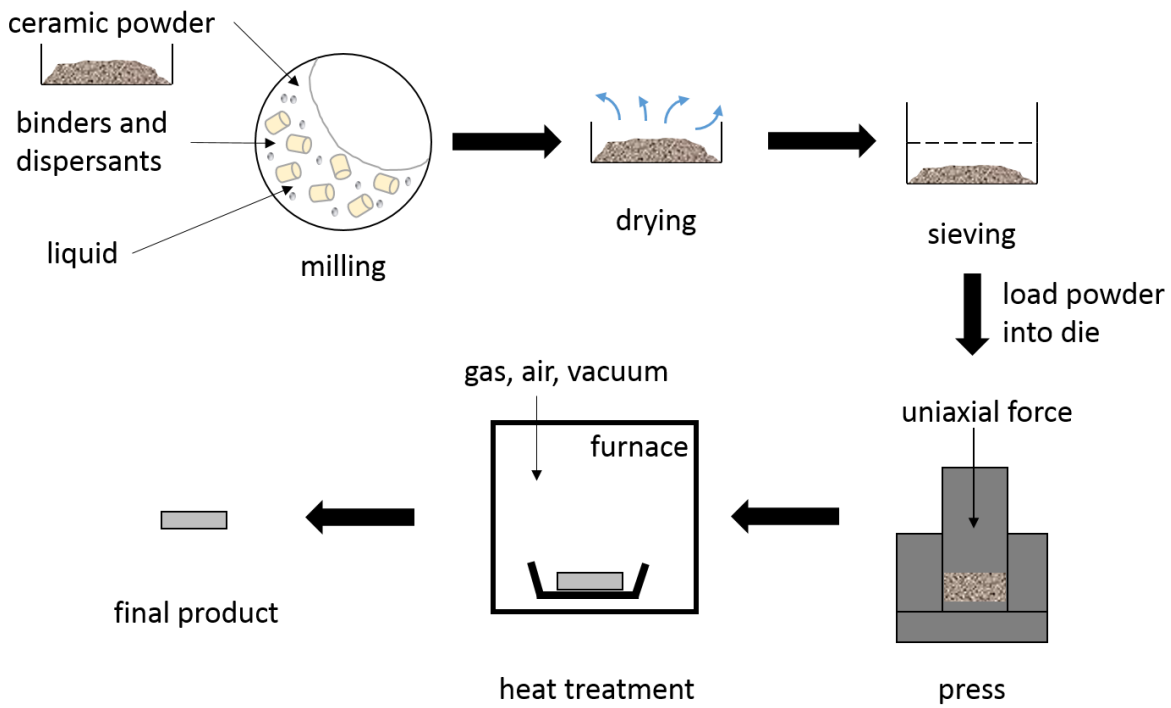

Figure 1: Steps involved in a typical conventional ceramic processing route. The top row of activities represent powder processing steps, which may not be carried out if the powder is suitable for pressing and heat-treatment as-purchased.

2.2 Sintering mechanisms

Sintering is a diffusion-controlled mechanism where atoms move from their original positions to the neck region between particles in order to fill gaps within the original structure and so transform the

material from the green state (non-joined particles in contact) to a contiguous body [14]. Matter can be transported to the neck region by six distinct processes. Diffusion along the surface, through the lattice, or by vapour transport can transport matter from the surface of the original particles to the neck region; alternatively matter can be taken from grain boundaries and moved along the grain boundary, where there is usually more space for movement, or through the lattice to the neck. Finally, if dislocations are present in the material these provide more space for diffusion to occur, allowing another route of matter transport to the neck region. The contributions of each of these mechanisms to the overall densification depends on the material composition, the density of grain boundaries and dislocations in the material, and the temperature at which densification is being attempted. In addition, densification only occurs where the matter transport mechanism acts to move the centres of the particles closer together such as bulk diffusion through the lattice; mechanisms which do not achieve this (*e.g.* evaporation of the material and surface diffusion) cause coarsening and reduce the surface energy. A more detailed discussion of the kinetics and thermodynamics of the sintering process can be found, for example, in Chapter 5 of Chiang *et al.*[11].

2.3 Regimes of densification behaviour in ceramics

During sintering the densification rate as the density of the material approaches the maximum level. This is because as densification proceeds, the surface area reduces and therefore fewer matter transport mechanisms can act [11]. In addition where the material has high grain boundary energy, densification must overcome a higher thermodynamic barrier to proceed [14]. In addition if gas is present in the pores of the material the densification is limited by the diffusion rate of the gaseous species through the lattice of the material which can be extremely slow [15].

Sintering can be divided into three regimes, which were first described by Coble in two papers published in 1961 [16,17] and which are illustrated in Figure 2. In the initial Stage I the particles begin to coalesce, with necks forming between particles. Grain growth does not occur until Stage II, where densification occurs such that the assembly of individual particles is transformed to a

contiguous body containing a continuous pore network. By the beginning of Stage III the pores are isolated at the corners of the grains which have formed from the original particles, at which point densification becomes much slower. The grain size increases with increasing density [11]. The sintering rate is directly proportional to the temperature of the sample, as more densification mechanisms are activated as the temperature increases. Lattice diffusion has a higher activation energy than grain boundary or surface diffusion [11]. As a consequence, high temperatures of 50-70% of the melting temperature are generally required for the densification of ceramic materials [18].

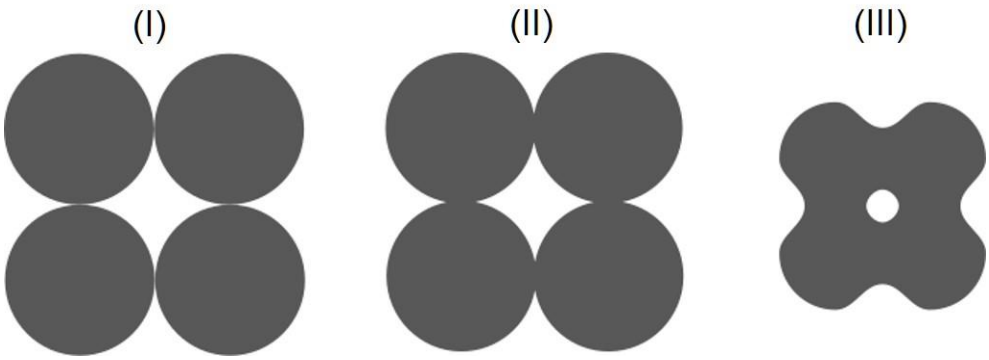

Figure 2: Stages of densification in ceramic materials. (I) initial stage – particles bond together, (II) intermediate stage – particles form a continuous network and shrinkage begins, (III) final stage – isolated pores remain, densification rate slows – significant shrinkage has occurred.

2.4 Microstructural changes observed during sintering

As the densification rate slows considerably through Stage III sintering, there is generally little advantage in using extremely long sintering times to gain dense specimens, as the increase in grain size diminishes any advantage of the small increases in densification achievable at this stage. Better results may be obtained by changing the atmosphere used during heat treatment, by increasing the temperature, or by the addition of dopants which change the grain boundary mobility [11]. In addition it should be noted that the presence of liquid-forming additives, even in very small quantities entirely feasible by slight contamination of the starting powder, can increase diffusion rates along the grain boundaries by allowing liquid-phase diffusion rather than the slower solid-state processes only [12].

Densification can also lead to undesirable abnormal (or discontinuous) grain growth during Stage III sintering, particularly in alumina, where some grains grow extremely to extremely large dimensions compared to others, weakening the overall structure [11,16]. The reason for this is not fully understood, though recent work has suggested that defect states called “complexions” found at the grain boundaries may play a key role [19]. Equally, coalescence of fine porosity can lead to the formation of large pores during the later stages of sintering, which can be extremely difficult to remove [12].

3. Flash Sintering Methods

The optimal conditions for flash sintering have not yet been sufficiently established to the extent that a “standard” configuration of apparatus exists. Rather different research groups have carried out flash sintering studies using various methods of heating the samples and applying the electrical voltage, monitoring electrical field conditions and shrinkage during the tests, and also different geometries of samples and electrode attachment methods. Apparatus is home-made or modified from commercially available instruments such as spark plasma sintering machines or dilatometers. In this section these methods will be described and compared in terms of flash sintering performance, advantages and limitations. In addition, sample geometry, the methods and materials for making electrical contact, and industrial techniques developed to date will be described. Finally flash sintering will be compared to other field-assisted sintering mechanisms in terms of the above factors.

3.1 Flash sintering apparatus

In its most basic form, a flash sintering apparatus consists of a high-temperature furnace and a power supply attached in some way to a ceramic sample. Additional monitoring equipment is required to determine the voltage, current, and sample displacement/shrinkage during the heat-treatment. From the literature to date, three main types of flash sintering apparatus have been identified. Representative schematic diagrams based on typical designs are shown in Figure 3.

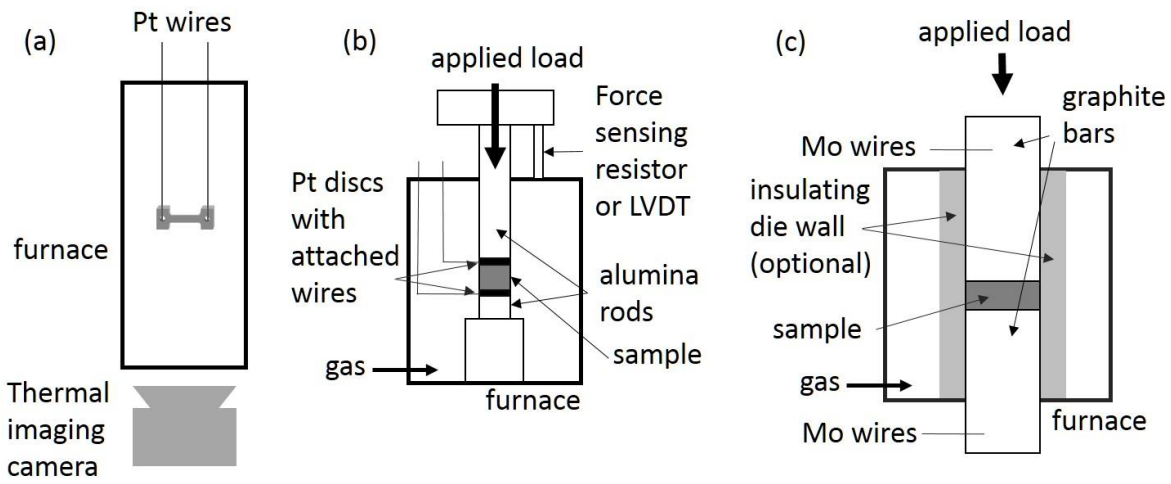

Figure 3: Flash sintering apparatus configurations. (a) vertical tube furnace with dogbone sample; (b) adapted dilatometer/mechanical loading frame; (c) flash spark plasma sintering / adapted hot press.

The first approach uses a vertical tube furnace with the dogbone-shaped sample suspended horizontally from the platinum wires which also serve as the electrodes [20–23]. These are threaded through the top of the furnace and connected to the power supply. Current and voltage monitoring devices are included in the power circuit. At the base of the tube furnace a camera with suitable filters can be pointed up the tube to directly record the shrinkage in the sample during flash sintering [20]. Variations on this approach include the use of a box furnace with a window in the door [8] and an adapted furnace for use during *in situ* X-ray diffraction experiments [23].

The second approach uses an adapted dilatometer [24] or mechanical loading frame [25], or similar home-built devices [26]. In this case some degree of loading is required to keep the sample in place, though generally in these setups the applied uniaxial force has been kept very low. A pellet-shaped specimen is placed between two electrodes usually made of platinum and supported by alumina push-rods. This is mounted in a furnace, such as a dilatometer chamber or a split-furnace on a mechanical testing frame. The power supply is attached to the electrodes by attached wires attached. Visualisation of the sample is not generally attempted in this case; densification is instead monitored by use of displacement sensors.

The third approach is most similar to a spark plasma sintering or hot pressing apparatus in design. This approach has been employed in both flash spark plasma sintering [27–31], where a commercial spark plasma sintering apparatus is used without the usual graphite mould and with high heating rates, and in a home-built approach using an induction furnace [32]. Uniaxial pressure can be applied at minimal or higher levels to maintain contact. In this setup the ceramic powder is loaded into an insulator-lined die and the electrodes are the top and bottom graphite plungers, an approach originally described by Zapata-Solvas *et al.* [33]. These are attached directly to the power supply. In this case the flash sintering cannot be visualised during the process and the detection of flash sintering relies either on observing the power surge or on detecting the change in displacement of the die.

One of the biggest challenges in flash sintering is the accurate measurement of sample temperature, and this is likely to account for some of the at times significant differences between flash sintering conditions described by different research groups. Reasonable efforts are made to measure temperatures close to the sample, but this varies according to the apparatus design and the temperature varies with even small distances from the sample surface. The use of optical pyrometers [34] can be helpful but are not suitable for use with all experimental configurations. In any case, the temperature at the centre of the sample could be considerably different to that at the surface, to say nothing of the variations expected on a local level due to variations in grain boundary energy. In light of this, in this review the processing conditions will be primarily discussed in terms of the *furnace* temperature at which flash sintering was seen to commence. In Section 5 methods of modelling the actual sample temperature during the flash sintering process and the implications of this for the underlying mechanisms of flash sintering will be discussed.

3.2 Specimen Geometry

Ceramic materials moulded into bars [35] and dogbones [20] with rectangular cross-sections and pellets of various diameter to height ratios [36–38] have all been flash sintered (Figure 4). Flash sintered samples generally have small dimensions [28]. As the voltage and current supplied by lab-

scale power supplies are relatively low, controlling the dimensions of the samples is one facile route to controlling the maximum electric field and current density. The initial (maximum) electric field can be calculated as $E_o = V/l$ where V is the voltage and l is the length of the sample between the electrodes, *i.e.* the length of the gauge section in a dogbone or the thickness of the pellet. This means that the initial electric field can be increased by using longer or thicker samples, even if the voltage is limited. The current density J is calculated as $J = I/\pi r^2$ where I is the current and r is the radius of the pellet or as $J = I/wd$ where wd is the cross-sectional area of the dogbone or bar. This means that the larger the radius of the pellet or the thicker and wider the dogbone, the smaller will be the current density passing through the sample. To enable the highest electric field strength and largest current density all dimensions of the sample should be made as small as possible. However this brings into question the relevance of the flash sintering processing route to larger scale samples more typical for real applications. To date there is no systematic examination of the effect of sample dimensions or shape on flash sintering in the literature.

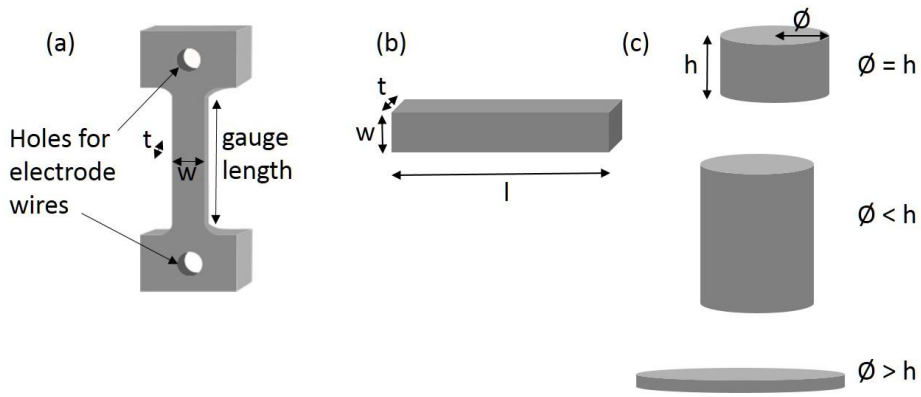

Figure 4: Specimen geometries used in flash sintering studies (references indicate examples of papers where these shapes were used). (a) rectangular cross-section dogbone (e.g. in [20]*); (b) rectangular bar (e.g. in* [35]*); (c) pellets, of various height:diameter ratios (e.g. in* [36–38]*).*

Dogbone-shaped specimens are convenient for the monitoring of shrinkage in the gauge section during the flash sintering process by visual methods [39], whereas shrinkage in pellets is usually measured using linear displacement techniques such as the use of a force sensor [26] or laser system [40]. There is evidence that the handle-sections of flash-sintered dogbone specimens

experience higher electric fields and hence higher temperatures, leading to larger grain growth under DC electric fields [41]. This means that in practice, were the samples to be used for further applications, these sections would need to be removed. It has also been suggested that drilling holes into the ceramic dogbone samples in the green state for electrode wires can introduce damage [41].

Dogbone-shaped samples have no practical applications [28], but the abnormalities observed in the microstructure of these samples away from the gauge section has important implications for future flash sintering of ceramics with more complex geometries. In addition, for disc shaped samples it is likely that larger dimensions would be required for practical applications. Thermal gradients are more likely in larger samples, which would lead to inhomogeneous densification. In part to investigate this, the group of Mike Reece at Queen Mary University of London [27,28,30] have developed a method called "flash spark plasma sintering" which uses commercial spark plasma sintering machines but with significantly higher heating rates akin to those experienced in flash sintering. Using this method silicon carbide discs up to 60mm in diameter have been densified at low furnace temperatures (1600°C) compared to conventional sintering (>2000°C) [28].

3.3 Electrical contact

Most electrodes used for flash sintering have been composed of platinum metal (in the form of ink, paste, and/or wires and plates) due to its high melting temperature and good electrical conductivity. While occasionally studies have been completed which use alternative electrode materials such as molybdenum wires [32] or copper wire [42], on the whole the choice of electrode material is not justified or varied systematically. Two studies where different electrode materials were used in the same study give some insight. Caliman *et al.* [43] used both silver and platinum ink applied over the surfaces of disc samples of β-alumina ($MgNa_2Al_{10}O_{17}$). In this material, no flash sintered occurred when using the platinum, due to the incompatibility between the sodium-ion conducting β-alumina and the platinum metal. The use of silver electrodes did result in flash sintering. This indicates the importance of electrode material choice when attempting to flash sintering new materials. In a recent

study by Biesuz and Sglavo [44] the flash sintering of α-alumina (Al_2O_3) was studied using platinum, carbon and silver pastes applied to the ends of dogbones. These regions were then attached to a power supply using the usual platinum wires. It was found that the onset temperature for flash sintering for a given electric field was lowered by some 250ºC when silver paste was used, with the highest temperatures observed for the use of platinum paste [44]. This was attributed to a reaction at the alumina/electrode interface catalysed by the silver and carbon which improved the conductivity of the material [44]. Platinum is a non-reactive noble metal so would not be expected to induce this effect [44]. This study indicates that while the melting temperature of the electrode material is an important consideration, other factors such as the potential to enhance the conductivity of the material should also be considered when designing a flash sintering setup.

In the case of approaches using modified spark plasma sintering machines and other furnaces, graphite electrodes are often used. In their paper examining spark plasma sintering of zirconium diboride, Gonzalez-Julian *et al.* showed that the use of graphite discs often placed between the ceramic sample and the graphite punches in spark plasma sintering can cause a reduction in current flow though the specimen [45]. The largest currents are obtained when the ceramic is pressed directly against the graphite to which the power supply is connected, giving samples with the highest density and largest grain size [45]. However this risks adhesion of the sample to the graphite bars, which is usually avoided by the use of the graphite foil which can be more easily ground off after heat treatment.

The method by which electrodes are attached to the ceramic sample is largely dependent on the specimen geometry. In the case of dogbone samples, electrode wires are placed through holes made in the dogbone handle regions [20]. Wires twisted around each end are used for rectangular bars [46]. The electrodes used for pellets are usually platinum discs placed against the top and bottom surfaces [47] with wires to the power supply attached. Alternative approaches are to attach the wires to meshes of platinum wire placed in the same position as the discs [24], to paint the top and bottom surfaces of the discs with conductive paint/paste (often platinum [48], but silver has also been used [49,50]), or to sputter coat each side of the discs with platinum [51]. Finally, Saunders *et al.* [52] have

described a flash sintering approach which used arc plasma electrodes rather than any additional material to realise a contactless setup, and successfully fully densified B_4C and SiC/B_4C composite materials. This technique simplifies the process, but causes considerable heating in the samples which can cause deleterious effects such as excessive grain growth and microstructural inhomogeneities.

As the methods of electrode attachment are generally dictated by the sample geometry and the apparatus configuration there is little systematic comparison of the different approaches within the literature other than the study of Caliman *et al.* [43] and Biesuz and Sglavo [44] described above, which only considered changes to the electrode materials. As there are simultaneously other significant variations between the flash sintering apparatus used by different groups, such an analysis is difficult to establish from reviewing the literature. If flash sintering methods are to be optimised for use with a wide range of materials, the issue of electrode material choice and electrode attachment method should be investigated further.

3.4 Industrial development of flash sintering techniques

Flash sintering has attracted considerable interest from the ceramics industry since it was first discovered. In particular, Lucideon [10,53], based in Stoke-on-Trent, United Kingdom, started to develop a large scale flash sintering kiln in 2011. This kiln, installed in 2013, uses convertible electrodes placed above and below the sample, which is placed on 25m-long rollers, to carry out flash sintering on a large scale [53,54]. While this kiln is still in development, it represents the first attempts at flash sintering on a large scale, supported by research in the literature and the development of processing maps for traditional ceramic materials [55] not previously flash sintered. Work by Lucideon has already shown that 15x15cm whiteware tiles can be flash sintered, albeit in a scaled-down process [56].

Flash spark plasma sintering (FSPS) is already carried out in commercial spark plasma sintering machines, and samples up to 60mm diameter have been produced already using an SPS machine based at Kennametal Manufacturing Ltd. in Newport, South Wales [28,57]. Like SPS and

hot pressing, FSPS will necessarily be limited to small number of samples for each run, however the speed of the process and the energy savings possible compared to conventional sintering of materials such as silicon carbide may well outweigh the disadvantages for high-stakes applications such as ceramic armour.

Further developments in industrial scale flash sintering are expected as understanding of the key parameters and limitations are established. However, as stated in the first paper to describe flash sintering, history tells us to expect a period of 10-20 years from discovery before such developments are incorporated into standard ceramic processing routes [4].

3.5 Comparison to other non-conventional ceramic firing techniques

Flash sintering is not the first sintering route developed for ceramics which uses electric field to enhance sintering rates. Microwave sintering uses microwave frequency (*ca.* 300MHz-300GHz) electromagnetic radiation to sinter ceramic materials at temperatures below conventional sintering temperatures and in short sintering times [58]. Ceramics produced by microwave sintering have high density and small grain size [59], though the mechanisms for the evolution of the microstructure during densification are not well understood [58] and extensive modelling efforts are in progress. It has been suggested by some researchers that densification during flash sintering occurs by a similar mechanism to microwave sintering [60,61]. Efforts to understand the relationships between the two processes include the development of the rapid "flash microwave sintering" carried out by Bykobv *et al.* for ytterbium-doped yttrium lanthanum oxide [62]. Flash sintering is usually carried out under DC electric field conditions [20], or AC fields in the low radio frequency range (up to *ca.* 1000Hz) [24].

In the field-assisted sintering technique (FAST) also called spark plasma sintering (SPS), the ceramic powder is placed inside a graphite mould, pressed with graphite plungers and a DC current is passed through the sample and the die, heating the sample to high temperatures in short time periods while under uniaxial pressure [63]. The mechanism for densification in this process is the subject of some controversy. Early work by Tokita suggested that the densification occurred due to "sparks"

forming between particles due to a plasma generated by the SPS apparatus [64], though later experimental work by Hulbert *et al.* disputes this [65]. In many cases there is little difference between hot pressing (where heat is supplied by an induction furnace rather than electric current through the die) and spark plasma sintering [66], with the advantages of the later chiefly originating from superior heating rates and higher applied pressures [1]. The exception is where materials have significant electrical conductivity, such as doped zinc oxide, where current-induced microstructural features can be observed [67].

FAST and SPS are essentially the same technique [68], though of course commercial equipment developed by different companies differs in aspects such as tool geometry, the application of electric current pulses, and methods of measuring the temperature. Langer *et al.* [69] have identified differences in the sintering behaviour of alumina and zinc oxide samples sintered in FAST and SPS machines, though noticeably no such difference was observed for 8YSZ.

Compared to both these techniques, flash sintering involves higher electric fields (*i.e.* higher voltages) passed directly through the sample. A much faster increase in the sintering rate is accompanied by a power surge [20]. Flash sintering typically occurs within seconds [20], whereas hold times in SPS and FAST are of the order of minutes [27]. However the actual process of flash sintering can be considered to be a modification of the field-assisted process described above. Flash sintering has been carried out using applied pressure (flash sinter-forging [37]) and in a spark plasma sintering machine without the usual graphite mould (flash spark plasma sintering [27]). Behaviour similar to that seen in the FAST process is observed in flash sintering experiments at low electric fields (even without applied pressure), and there is sometimes an observed transition between FAST behaviour and flash sintering [20]. For clarity in this review and in line with the flash sintering literature, the term spark plasma sintering (SPS) will be used to refer to the established technique, whereas FAST will be used only in describing behaviour observed during flash sintering tests which is akin to that observed under the usual FAST/SPS conditions, albeit without using applied pressure or graphite electrodes.

4. Flash Sintered Materials

While early studies of flash sintering focused almost exclusively on zirconia, flash sintering has now been demonstrated in a range of ceramic materials, including structural ceramics, ferroelectric materials, materials for use in solid oxide fuel cells, and composites. Studying materials with different ionic and electronic conductivities in particular sheds new insight on the flash sintering mechanisms in ceramic materials. In the sections below, the flash sintering conditions established for these materials are described and discussed.

4.1 Zirconia

Zirconia, an ionic ceramic, is by far the most extensively studied material in the flash sintering literature, attracting extensive attention due to its proven ability to undergo flash sintering under suitable electric field and furnace conditions, having been the subject of the first paper describing the phenomenon by Cologna *et al* [20] in 2010.

Under equilibrium conditions at room temperature and pressure it has a monoclinic crystal structure, however the addition of small amounts of additives such as yttria (yttrium oxide) stabilises the high temperature polymorphs. 3-mol% yttria added to zirconia will give a tetragonally stabilised form at room temperature, while 8 mol% yttria stabilises the cubic form of the polycrystal [12]. Such compositions are available pre-mixed with nanoscale grain size from commercial suppliers such as Tosoh (Japan), and these materials have been extensively used in flash sintering studies. With enhanced toughness compared to non-stabilised zirconia, 3Y-TZP finds applications in dental implants and ball milling media [12]. 8YSZ is a commonly used material in the electrolyte of solid oxide fuel cells [4].

Studies on flash sintering of zirconia have used all three of the standard sample shapes identified in Section 3.2. The large number of flash sintering studies carried out using 3Y-TZP or 8YSZ enable us to draw somewhat clearer conclusions about the behaviour of these materials compared to some others which have been less extensively studied by different research groups.

Flash sintering was first observed in 3Y-TZP by Cologna *et al* [20] in 2010. However this work grew from an extension of earlier studies by the research groups of Rishi Raj at University of Colorado, Boulder [70] and Hans Conrad of North Carolina State University [5,7] on using electric fields to suppress grain growth in 3Y-TZP ceramics. In the earlier studies, modest initial electric fields (both AC and DC, of up to 18.5V/cm) applied to zirconia ceramics during sintering were shown to repress grain growth. Cologna *et al*'s 2010 study [20] used higher initial electric fields above 40V/cm which caused a rapid enhancement in sintering rate in 3Y-TZP at 950ºC in dogbone samples. The characteristic power surge indicative of flash sintering was observed for the first time (example shown in Figure 5) and full densification was achieved in less than 5s [20].

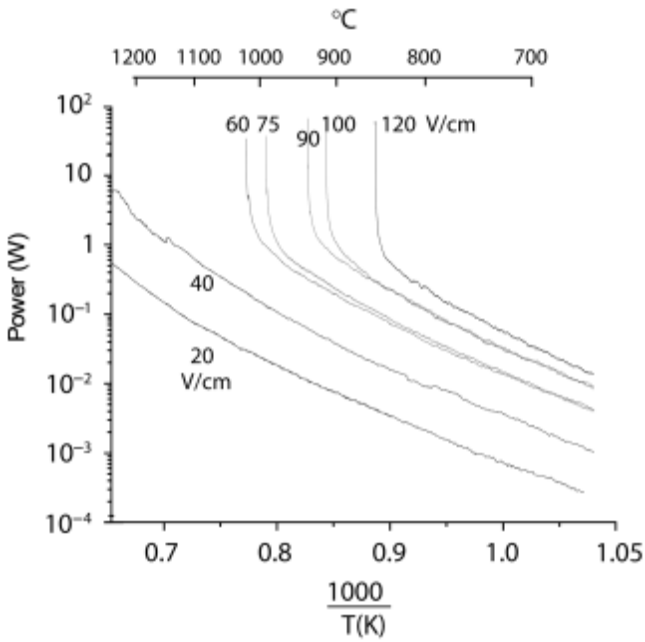

Figure 5: Temperature-power relationships for 3Y-TZP undergoing flash sintering for electric fields of 60V/cm and above. The flash sintering power surge is shown as the near vertical lines at higher temperatures. For these samples flash sintering did not occur for samples exposed to only 20 or 40V/cm. Reproduced with permission from Cologna et al. [20].

3Y-TZP is the material which has so far been most widely studied in the flash sintering literature. While initial studies focused on establishing the parameters for the flash sintering technique, many later studies have focused on producing supporting evidence for theories that explain why flash sintering occurs in particular materials and under particular conditions. Some of these

studies will be described in greater detail in Section 5 below, where the proposed theories are compared.

While in Cologna *et al*'s initial paper, conditions of 120V/cm DC with 850ºC flash sintering onset furnace temperature were identified as the optimal flash sintering conditions for 60nm commercial 3Y-TZP powders [20], later studies have revealed the effect of more variation in the flash sintering conditions and the material properties. Samples have been flash sintered in dogbone [8,20,22,23,39,41,71–73] and pellet form [26,31,36,37]. The apparatus used includes a vertical tube furnace with camera to detect shrinkage in dogbone samples [20,22,39,41,71,72], a box furnace with front window for use of a camera [8], a commercial spark plasma sintering machine used without the usual graphite mould [31], a vertical furnace adapted to hold pellets by the use of alumina supporting bars with [26,37] or without [36] significant applied load, and a modified system holding suspended dogbones designed for *in situ* X-ray diffraction studies [23,73].

Both AC [41] and DC [37] fields have been used in the flash sintering of 3Y-TZP though no comparative studies have been carried out within the flash sintering regime with a wide range of electric field strengths. Although these experiments were not carried out in the flash sintering regime, Conrad and Yang [22] studied the effects of AC and DC fields of up to 55V/cm on density and grain size. The results showed that the use of AC fields resulted in lower grain sizes for a given electric field strength, along with lower temperature for the same densification.

Initial experiments on flash sintering of 3Y-TZP used a continuously increasing heating rate, such that the onset furnace temperature was determined by correlation with the shrinkage rate or power surge [20]. However flash sintering can occur under isothermal settings, albeit often after an incubation time. Examined in detail for the first time by Francis and Raj [39], this finding demonstrated the importance of the maximum current in determining flash sintering properties. In these experiments the power supply was only turned on once the sample was determined to have equilibrated with the furnace temperature. The current limit of 60mA/mm^2 with an electric field of 100V/cm at 900ºC resulted in flash sintering after 15s. For lower electric fields this incubation time increased significantly to up to 2500s for a hold temperature of 700ºC, electric field of 125V/cm. The

degree of densification varied in the samples, with the densest samples achieved for higher current densities. These findings have important implications for the design of flash sintering experiments which do not always appear to be heeded in later studies, where often the power supply is switched off after a relatively short period of time if flash sintering has not occurred. They also suggest that a combination of electric field (affected by voltage and sample size), current density (affected by the current and sample size), and the furnace temperature can all affect the final density of the flash sintered material.

The addition of uniaxial stress to the flash sintering process is commonly described as flash-sinter-forging, as a modification of the sinter-forging process whereby the sample under pressure is able to freely deform in the radial direction [66]. This process, as described by Francis and Raj in 2012 [37], involves a pellet-shaped sample with electrodes placed against the faces of the pellet using a fairly modest uniaxial stress up to 12MPa. It was shown that the stress reduced the onset temperature for flash sintering, with a sample which flash sintered at 915ºC under 1.5MPa undergoing flash sintering at 850ºC under 12MPa, under the same conditions of electric field. This has positive implications for future developments of flash sintering processes using non-suspended samples, which are perhaps rather more applicable in the industrial context.

Most of the 3Y-TZP flash sintering papers in the literature use nanocrystalline powders with little difference in quoted particle size. The effect of varying the particle size have been systematically investigated by Francis and Raj [72]. Flash sintering was observed at 920ºC for 1μm average particle size powder at 100V/cm, with 955ºC for 2μm, 990ºC for 5μm, and 1040ºC for 10μm. However only the sample consisting of 1μm particles reached a density above 90% despite starting with the lowest green density. These results indicate that the conductivity of the powder compact is important in determining the flash sintering behaviour, as the large-particle green compacts have lower conductivity than those composed of smaller particles, due to a greater number of contacts between the particles [74]. This finding is an additional consideration for flash sintering, indicating that higher degrees of densification will be attained if the conductivity of the green compact is maximised. It is also worth noting that while the particle sizes stated were in the micrometre range, the authors

acknowledge that the particles were made up of smaller crystallites agglomerated into particles. Given the propensity of nano-sized powder ceramics to agglomerate [75], it may be necessary to mill and disperse particles before flash sintering in order to optimise the green compact properties.

The measurement of grain size in flash sintered samples is often absent or only briefly dealt with in studies of flash sintering. This is perhaps reasonable as there are many factors which affect grain size; in particular the length of any isothermal hold before, during or after the flash event can cause considerable changes; in addition there can be differences in grain size in different regions of the sample. Full characterisation of the grain size of ceramic materials is a time-consuming analysis which is rarely carried out unless it is the main focus of a study. The evidence suggests that the grain size of flash sintered 3Y-TZP sintered to full density is fairly similar to that of conventionally fully sintered 3Y-TZP [71], even though the temperatures and time for flash sintering are lower than for the conventional methods. This is illustrated in Figure 6 , reproduced from M'Peko *et al.* [71], where conventional and flash sintered 3Y-TZP samples are compared. However like-to-like comparisons of the conditions of different flash sintering conditions is more difficult given the limited data available, particularly as in early papers the importance of the current density was not anticipated and this is often not reported. One interesting observation with important ramifications was made by Qin *et al* [41] in looking at the grain size distribution within the microstructure of flash sintered 3Y-TZP. Using dogbone-shaped samples with platinum wire electrodes attached through holes in the wider region at each end of the gauge section, the material was flash sintered to at 900ºC with 100V/cm electric field and 50-100mA/mm^2 current density limit, and a hold time of 2-60s. Significant differences were found in the grain sizes near the cathode and the anode regions, with those near the anode end having an average grain size of around 1μm, while the grain size rose to around 25um near the cathode end for the longer hold times under DC conditions. As the effect was not observed when AC conditions were used, these differences were attributed to the accumulation of vacancies at the cathode end. DC current also resulted in an inhomogeneous electric field near the handles of the dogbones. Temperature variations are also observed in the models of Grasso *et al* [76] who note a difference in sample temperature of ~500ºC between the handles of the dogbones and the gauge section under

120V/cm and a furnace temperature of 850ºC. Finite element electric field and temperature modelling will be essential as flash sintering is expanded to more complex geometries than the dogbones and pellets used to date, as the grain size growth due to higher temperatures caused by regions of higher electric field due to sharp corners and similar geometric features may cause weaker regions with larger grain size.

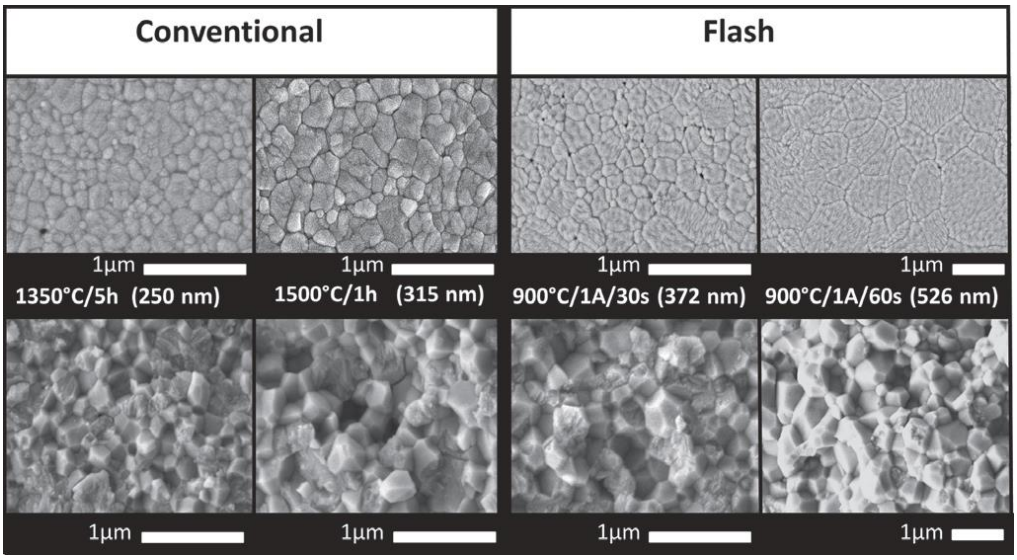

Figure 6: Comparison of grain size determined from polished surfaces (top row) and fracture surfaces (bottom row) of 3Y-TZP samples prepared by conventional and flash sintering. Reproduced with permission from M'Peko et al. [71].

Clear evidence of ion motion during flash sintering is presented by Lebrun *et al*. [23], who observed a partial phase change in high-resolution *in situ* X-ray diffraction studied carried out at the Advanced Photon Source. The new phase, characterised by a peak lying between the (112) and (200) diffraction peaks of tetragonal zirconia, appears while the power supply is under current control (depending on the current limit) during the latter stages of flash sintering (Stage III) and vanishes over a period of time (10-30 minutes) after the power is switched off. These observations suggest that the phase originates from concentrations of defects which then diffuse apart after the power supply is switched off. The importance to the flash sintering process of space charge due to the yttrium ions in the grain boundaries has been described by Conrad [77], who described how the space charge and electric field interact to retard the grain growth in 3Y-TZP. M'Peko *et al.* [71] examined the defect

chemistry of 3Y-TZP after flash sintering through measurements of the dielectric properties. The observed behaviour was analysed by examining the charge diffusion in the 3Y-TZP mediated by defects. It was found that the grain boundaries in flash sintered samples were narrower by 30% than in conventional sintering, and the grain boundary conductivity was higher in flash sintered samples than conventionally sintered samples. Therefore the flash sintering process is found to change the densification behaviour by making diffusion of material easier along the grain boundaries. The concentration of oxygen vacancy defects at the grain boundaries was found to be higher in flash sintered samples than conventionally sintered samples, suggesting that flash sintering in 3Y-TZP is, at least in part, a defect-mediated process, and that the retardation of grain growth is largely due to the magnitude of the applied current rather than the strength of the electric field [36].

8YSZ has been comparatively less extensively studied than 3Y-TZP. Both dogbone shaped samples [4] and pellets [25] have been successfully flash sintered, using both Pt wire electrodes to suspend the dogbones [4,21] and the Pt discs/grids or paint electrodes for pellets [24,25,38,47,78,79]. A variety of experimental apparatus setups have been used, including the vertical tube furnace with suspended dogbone construction [4,21], an adapted dilatometer [38,47,78], a standard tube furnace [24], a split vertical furnace mounted in a mechanical testing machine [25], and a custom-built vertical arrangement with pellet shaped samples, with the ability to add load [79]. Both DC [21] and AC [38] conditions have been used for densification. These papers have demonstrated flash sintering in 8YSZ under a range of different conditions, though full densification is not always achieved during the flash. While the data available is somewhat limited, and often does not allow comparison, an attempt at analysing optimal conditions has been made. The initial electric field strength is reasonably monotonically related to the flash onset temperature as shown in Figure 7, regardless of whether the power supply is AC or DC. It is noticeable that for 8YSZ current flow is extremely important in the flash sintering process. Kim *et al.* [80] exposed already consolidated 8YSZ samples to electric fields and noticed a difference in the grain size at the cathode compared to the anode in pellet-shaped samples. This was attributed to a gradient in the concentration of oxygen vacancies across the sample. Steil *et al.* [79] used “hyper-flash” sintering using a high initial power spike over a short time period

to show that high levels of densification to 80-90% could be obtained within 1s. This spike causes a reduction in the sample's resistance and therefore rapid shrinkage occurred along with a rapid sample temperature increase. Spikes can also be applied consecutively ("double-flash") to obtain further degrees of densification [79], indicating that processes causing the flash sintering are not depleted by flash sintering occurring. Baraki *et al.* [25] held the temperature at 1200ºC for 120 minutes to obtain a 10% increase in the bulk density compared to that immediately after sintering in the FAST regime. However it is noticeable that samples flash-sintered under high current densities did not undergo further densification during the isothermal hold, suggesting that the driving force for densification is reduced by the electric current. Downs and Sglavo made observed that the current density must lie between 17.8 and 87mA/mm^2 in order for full densification to be achieved in 8YSZ [21], suggesting that a certain power threshold must be achieved in order to attain flash sintering. In recent work Du *et al.* [47] attribute the densification behaviour in 8YSZ to ionic conductivity increasing causing thermal processes triggered by Joule heating of the sample above the sample temperature. The current and the sample heating form a feedback loop whereby as the current increases, the more Joule heating occurs, leading to greater current flow. Clearly then the densification achieved will be dependent on the conditions under which the flash sintering is carried out. Where the power supply is limited to a certain maximum current, the Joule heating will necessarily be limited also, and hence the runaway process of flash sintering may enter a steady-state condition before densification is fully completed. In the work of Du *et al.* [47] the maximum current density was ~200mA/mm^2, significantly higher than stated in most flash sintering studies (where such information is provided). It should therefore be noted for future studies that according to this analysis, optimal flash sintering conditions may not be determined if the current density hits the maximum limit of the power supply during the process.

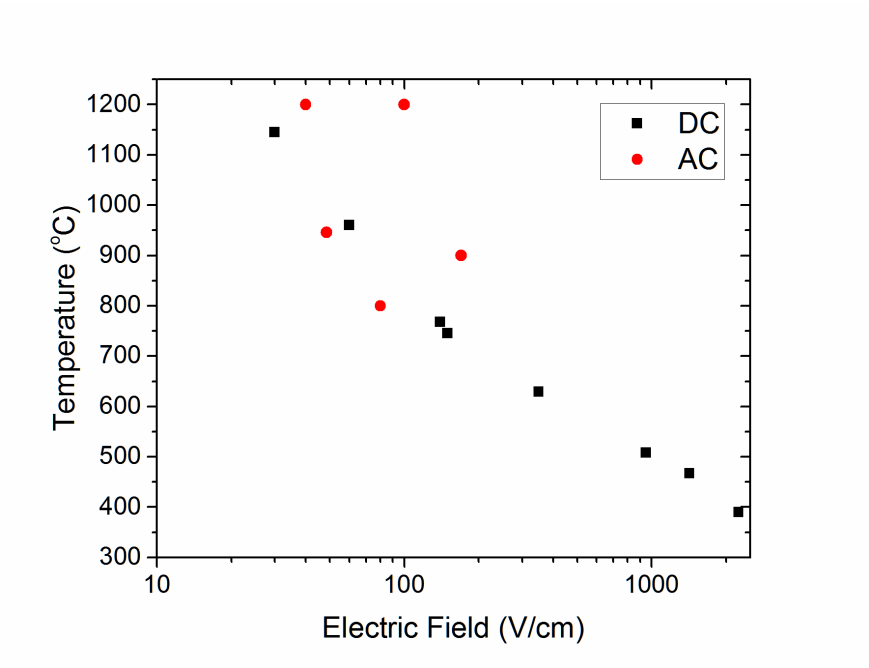

Figure 7: Relationship between the initial electric field and the flash onset temperature in the furnace for 8YSZ in AC or DC fields. Data was taken from [4,21,24,25,38,79].

4.2 Carbide and Borides

4.2.1 Silicon Carbide

Silicon carbide is a semiconducting, covalent ceramic material used in a number of applications including ceramic armour and electronics. Silicon carbide requires high temperatures and applied pressure to densify (>2000ºC) and sintering additives are often used. Two combinations of sintering additives are the "ABC" type (aluminium and boron carbide, though sometimes just boron carbide is used) and the "AY" type (alumina and yttria, which cause liquid phase sintering by forming yttrium aluminium garnet at high temperatures). The two main types of silicon carbide are denoted α-SiC and β-SiC, with α-SiC usually consisting of a mixture of the 4H and 6H hexagonal polymorphs, and β-SiC being solely the 3C (cubic) crystallographic structures. It is worth noting in the context of the few studies carried out on the flash sintering of SiC that these materials are known to have different sintering behaviours [12].

Silicon carbide flash sintering has been reported by two research teams to date, using different configurations of apparatus but always on pellet-shaped samples. Zapata-Solvas *et al*. [32], the first to report flash sintering in SiC, produced pellet-shaped α-SiC samples with ABC additives, AY additives, and additive-free. The apparatus employed an alumina-lined graphite mould (such that the current passed only vertically through the sample) placed in an induction furnace with minimal pressure applied (0.1MPa) to maintain contact between the graphite electrodes and the ceramic compact. Heat-treatments were carried out in flowing argon gas. All compositions of samples were shown to exhibit flash sintering behaviour, exhibiting a power surge during the sintering process. The lowest flash sintering "furnace" temperature (measured in the wall of the mould next to the sample) was 1029°C for the SiC samples with ABC additions under an applied field of 300V/cm; only a slightly higher furnace temperature was required for SiC with AY additions at the same applied field. However SiC with no additions required a furnace temperature at least 250°C higher for the same electric field. It is noticeable however that the maximum density (corrected for additive content) fell short of full densification, ranging from 56% for SiC with ABC additives at 10A to 88% for SiC with AY additives at 15A. Grain size measurements were not attempted but were of the order of 1-2um. Noticeable decomposition was observed in the fracture surface of the SiC samples using scanning electron microscopy. This decomposition was attributed to extremely high (2700-2800°C) temperatures being reached in the interior of the specimen; these temperatures being the decomposition temperature of pure SiC under atmospheric pressure, though of course pressure gradients within the sample may actually reduce the temperature required for decomposition locally within the material. The difficulty of truly understanding the temperature locally within the sample is again indicated in the difficulty of interpreting the behaviour of these samples.

α-SiC and β-SiC have also been studied by Grasso *et al* in two papers published in 2016 [28,30]. In both cases the silicon carbide samples were subjected to "flash spark plasma sintering" (FSPS), which uses a flash sintering setup within a spark plasma sintering machine, allowing significant uniaxial pressure to be readily applied, and with the ability to generate much higher currents (thousands of amps) compared to conventional flash sintering techniques. The DC current is passed

through the sample using the spark plasma sintering machine. Unlike in SPS the current passes only through the sample, not also through the walls of the graphite SPS mould. While this is undoubtedly a convenient approach, particularly given that SPS machines can readily operate under high vacuum or a range of gaseous atmospheres, and the chambers can accommodate larger samples, the parameters involve differ from those usually stated for flash sintering, making direct comparisons between the techniques difficult. Some observations are included here. Sintering was observed to occur very rapidly (in less than 1 minute) for samples of α- and β-SiC. Densities of the samples reached up to 96% for the sample which underwent FSPS at 10kW power. It is noticeable that at 1358ºC the temperature measured (taken to be the equivalent of the furnace temperature) involved were rather higher than those stated by Zapatas-Solvas *et al* [32]; however this may be due to the more accurate measurement of the sample temperature within the relatively well-enclosed commercial SPS set-up. The estimated sample temperatures were above 2000ºC for all samples, however there is likely to be considerable error in this value. The grain size was not determined. Some phase transformations were observed, particularly a transformation of some β-SiC to α-SiC polytypes, and in the later paper texture parallel to the pressing direction was clearly evident β-SiC with and with B_4C sintering additives, though noticeably high density was only achieved in 10wt%-B_4C-β-SiC samples [30]. Samples were processed as both 20mm diameter discs and 60mm discs, with uniform microstructures. While densification rates were clearly extremely rapid, there remains a question as to whether the mechanisms involved truly involve flash sintering, or are in fact a form of extremely well-controlled field-assisted sintering. It is noticeable that in a later paper using plasma electrodes, silicon carbide did not fully densify despite high power being applied for 60s [52]. This aside, it is clear that the FSPS process is scalable and rapid, representing a marked improvement on the already rapid SPS processing times.

4.2.2 Boron Carbide

Flash spark plasma sintering using the plasma electrode method described in Section 3.3 above resulted in fully dense boron carbide and boron carbide/silicon carbide composite material [52]. Boron carbide has also been sintered by the flash spark plasma sintering method by Niu *et al.* [29]. In this work an insulating mould was used so pre-sintering of the sample was not required. Using high currents of 2000A, B_4C with 99.2% density was produced at 1931ºC and 15.3MPa with a short hold time of 1 minute [29]. In comparison, densification of B_4C with no applied pressure required 2250-2350ºC [81], though with a high pressure of 80MPa, 1750ºC for 5 minutes were sufficient in conventional spark plasma sintering [82]. Under hot pressing conditions at 1950ºC, a similar temperature to that used in flash spark plasma sintering, over 1 hour at 30MPa pressure was required [83]. The grain size of the flash spark plasma sintered materials was 3.5μm, compared to a starting particle size of 2.36μm [29]. Using a higher pressure for flash spark plasma sintering more in line with those used in conventional spark plasma sintering [82] may result in a further lowering of the flash sintering temperature.

4.2.3 Zirconium diboride

Zirconium diboride is a high temperature refractory material with high electrical conductivity, giving it several potential applications including as high-temperature electrodes [84]. To date flash sintering of zirconium diboride has only been carried out using flash spark plasma sintering (FSPS) by Grasso *et al.* [27]. Pre-heat-treated ZrB_2 pellets of approximately 63.6% density were placed between graphite punches without a surrounding mould (in contrast to conventional SPS). Only a small uniaxial force (5kN) was used to maintain contact between the sample and the electrodes. Using a peak power of 25kW, the ZrB_2 powder was shown to densify to 95% of the theoretical maximum in 35s with a grain size of around 11μm. The grain growth was most significant for hold times above 25s, though in addition the density only reached a maximum of 85% after this time. The temperature measured from the graphite punch 4mm from the sample was 2198ºC at the maximum densification.

In comparison to the 0.2kWh energy consumed by the rapid FSPS, conventional SPS required around 4kWh of energy to densify a similar sample at 2100°C in 20 minutes hold time. However, while the authors rightly argue that FSPS has a number of advantages compared to the more established methods of flash sintering, there are limitations in that the samples required pre-sintering to obtain sufficient mechanical strength to undergo the process, and the grain size obtained was very large compared to that usually expected from SPS; a smaller grain size with a similar density can be obtained by SPS at higher pressures that those used for the conventional SPS in this work, for example see Zapatas-Solvas *et al* [85]. However there is scope to remove some of these disadvantages. For example, Gonzalez-Julian *et al.* [45] demonstrated that for field-assisted densification of ZrB_2 in conventional SPS moulds, where the maximum current is permitted to pass though the sample during heat treatment, the density is maximised. Using a modified SPS set-up where the sample is insulated from the graphite die walls using an insulating alumina tube inside the die, similar to the setup described by Zapata-Solvas *et al.* [32], thus forcing the current to flow through the sample rather than through the die walls, may more fully realise the advantages of the flash sintering setup within an SPS configuration.

4.3 Oxide Ceramics other than Zirconia

4.3.1 Yttria

Yttria ceramic is highly prized for particular applications due to its resistance to chemical attack, for example in hydrogen plasma applications [86]. However it is difficult to process, requiring either vacuum or a hydrogen atmosphere [86]. Yttria with crystallite size 20nm was shown to flash sinter without dopant additions by Yoshida *et al.* in 2014 [86]. Shaped into the form of a dogbone sample and held horizontally in a vertical tube furnace arrangement, the material undergoes a flash sintering onset at the lowest furnace temperature of 985°C under an initial electric field of 1000V/cm, and an electric current limit of 60mA, resulting in material with 97.9% density. The highest density sample in the study was obtained for a lower initial electric field of 500V/cm, with an electric current limit of

60mA, and higher furnace temperature of 1133ºC, which resulted in a sample of 99.6% density. The density and grain size both increased as the current limit increased. In all cases flash sintering occurred after a period of field-assisted sintering. This delayed onset is attributed to the lower electronic conductivity of Y_2O_3 compared to other ceramics such as 3Y-TZP.

It is noticeable that flash sintering in Y_2O_3 resulted in significant grain growth compared to conventionally sintered samples heated to the same or even higher temperatures, and also to those which were subjected to initial electric fields below the flash sintering limit of between 300-500V/cm at 60mA current limit (field assisted sintering, FAST) [86]. However the densest samples were produced by flash sintering with the highest current density limit used. This suggests that, for ytttria, if small grain sizes are required, low electric fields should be used (FAST regime), whereas if high density at low temperature is the priority, flash sintering at high electric field strength is required.

4.3.2 Alumina

Alumina is a widely used oxide ceramic which is typically sintered around 1600ºC, usually with added sintering aids such as MgO in order to reduce the instance of abnormal grain growth [11]. Flash sintering in α-alumina has been attempted by Cologna *et al.* in 2011 [87], Gonzalez-Julian and Guillon in 2015 [88], and Biesuz and Sglavo in 2016 [44]. The results so far show some contradictions. Cologna *et al.* [87] showed that 0.25wt% MgO-doped Al_2O_3 flash sinters to full density with an electric field of 500V/cm or above, with furnace temperatures of 1320ºC for 500V/cm and 1260ºC for 1000V/cm. These experiments used a continuous heating rate rather than an isothermal hold. The current was limited to 60mA, suggesting a maximum current density of around 10A/mm^2 in the dogbone shaped sample gauge section; however it is not clear whether this limit was reached during the flash sintering process, so the current density may in fact be somewhat lower.

Gonzalez-Julian and Guillon [88] employed a liquid-phase addition of calcium-aluminium-silicate (CAS) glass to aid the sintering process. In this case, the current passing through the liquid phase once molten above 1350ºC resulted in flash sintering occurring at the lower initial electric field strength of 150V/cm and with an onset furnace temperature of 1315ºC for samples with 10wt% CAS

glass addition. This sample reached a relative density of 98.58%. Other samples also sintered, but did not reach such high density and there is less evidence of flash sintering behaviour with strongly time-dependent sintering curves.

A more recent paper by Biesuz and Sglavo [44] examined in greater detail the effect of electric field and current density in flash sintering 99.8% alumina samples. For high fields (1500 and 1250V/cm) flash sintering was observed for current density of 2-6mA/mm^2 and no flash sintering behaviour was in evidence for 0 or 250V/cm electric fields. Between these conditions a mixed behaviour is seen, where field-assisted sintering is observed, followed by flash sintering once the sample reaches the current limit. However it is noted that full density is only achieved for samples flash sintered at 1000V/cm or high and 6-7mA/mm^2. For these samples flash sintering occurred at around 900°C for electric fields of 1500V/cm, increasing to 1000°C for 1250V/cm and 1070°C for 1000V/cm when using platinum electrodes. Lower flash sintering temperatures were observed for carbon and silver electrodes at the corresponding electric field strengths, however the use of silver electrodes in particular limited the degree of densification observed.

It is clear from these three studies that the impurity concentration is critical in determining whether alumina will successfully flash sinter in a given experimental set-up, however the nature of the impurity is critical. Cologna *et al.* [87] used >99.99% purity alumina, while Gonzalez-Julian and Guillon [88] employed a 99.7% purity powder, though these 0.3% impurities are not specified, this is actually a higher impurity level than the 0.25% addition of MgO made by Cologna *et al* [87]. Biesuz and Sglavo [44] state the impurity content of their 99.8% pure alumina, containing a total of 0.2% impurities including MgO, Na_2O, Fe_2O_3, SiO_2 and CaO. This level is similar to the 0.25% MgO in Cologna *et al.* [87] where flash sintering was observed. Clear variations in the electric field, current density and furnace temperature conditions required for flash sintering in alumina are seen between the studies by Cologna *et al.* [87] and Biesuz and Sglavo [44], despite similar purity of alumina samples, suggesting that either the impurity content is extremely critical, or that the setup of the experimental apparatus plays a key role. Further work is needed in this area to establish the critical aspects of impurity type and quantity on flash sintering behaviour in alumina.

Alumina exists in both α-alumina and γ-alumina forms, however of these only α-alumina has been shown to flash sinter to date. The somewhat confusingly-named β-alumina, which is actually sodium-aluminate e.g. $MgNa_2Al_{10}O_{17}$, a strongly ionic material used in applications such as solid oxide fuel cells, was flash sintered by Caliman *et al.* [43] using silver electrodes with electric fields of 120V/cm, furnace temperature of 550ºC, and maximum critical current of 10A/cm^2. These samples had relative densities of 88%, the highest achieved in the study. Interestingly, for this material platinum electrodes proved ineffective due to incompatible electrochemical reactions. This work demonstrates the importance of the understanding the diffusion rates and behaviour of ionic charge carriers in the material undergoing flash sintering, not just the electrical conductivity.

4.3.3 Titanium oxide

Titanium oxide is a valuable material for functional applications such as energy storage and sensors [89]. Flash sintering of pure titanium oxide in the rutile crystallographic form was first reported by Jha and Raj in 2014 [89]. Dogbone shaped samples were flash sintered with the use of platinum wire electrodes in a tube furnace heated to 1150ºC. Flash sintering occurred for initial electric fields of 250V/cm and above (maximum current density of 12 A/mm^2), with the lowest flash sintering furnace temperature occurring at 640ºC for 1000V/cm, leaving samples with a density of around 90% and grain size around 1.5μm. This is significantly lower than typical conventional sintering conditions of 1000ºC for 20h. Later experiments by Jha *et al.* [46] built on this work by examining the effect of electric field on pre-sintered TiO_2 samples using the Advanced Photon Source. The samples were monitored by X-ray diffraction while situated in a furnace at 800ºC, with an electric field of 100V/cm passing through the samples. The power supply current limit was 25mA/mm^2. While under the electric field it was found that the intensity of peaks due to the (110) and (111) crystallographic planes decreased, while that that of the (211) peak increased. This effect was reversible by switching off the DC power supply. These observations suggest that the TiO_2 unit cell distorts due to the electric field, and this may be associated with the accumulation of charged defects such as oxygen vacancies and

titanium interstitials. This experiment replicates conditions late in the flash sintering process (*i.e.* after the flash event has already taken place), so it may be that under initial flash sintering conditions this effect would not be measurable.

Most recently in 2016, Zhang *et al.* [90] studied the conditions for flash sintering of both anatase and rutile forms of TiO_2, with and without added dopants of nitrogen and vanadium. Shaped into thin pellets, the samples were heated within an initial electric field of 500V/cm. The maximum current density was around 20A/mm^2. Flash sintering occurred in all samples at furnace temperatures between 665-831°C, consistent with the findings of Jha *et al* [89] who saw flash sintering at 500V/cm and 700°C in undoped rutile TiO_2. Furnace temperatures were lower for the anatase samples that for the rutile samples; this is attributed to the higher electrical conductivity of the anatase phase. In all cases the anatase phase transformed to rutile during flash sintering, as would be expected under equilibrium heating conditions below 1100°C. The density of the samples was between 86% (V-doped anatase) and 97% (undoped rutile), with grain sizes between 0.21μm (N-doped rutile) and 1.11μm (undoped anatase). There was no correlation between density and grain size for these samples, though interestingly the three samples which had higher flash sintering onset furnace temperatures tended to have sub-micron grain sizes, while the three with the lowest flash sintering onset furnace temperatures all had grain sizes of 1-1.1μm.

Knaup *et al.* [91] used their simulations of the lowering of melting temperature in TiO_2 to partially explain some of the observed material behaviour in flash sintering. Their models show that the oxygen concentration of rutile TiO_2 decreases during heating, leaving oxygen vacancies which accumulate at the surface and enhance the conductivity. With an oxygen concentration gradient present in the samples, the melting temperature may differ significantly throughout the sample. While there is no microstructural evidence of the bulk melting of TiO_2 samples during flash sintering, none-the-less the local reduction in melting temperature may manifest as enhanced atomic diffusion rates, leading to enhanced sintering. This model-based hypothesis requires significant careful experimental work involving controlled oxygen atmospheres to verify these findings.

4.3.4 Tin dioxide

Tin dioxide is an n-type semiconducting material used in applications including chemical sensors [92]. However it is impossible to fully sinter without sintering additions, due to evaporation [93]s. Muccillo and Muccillo [94] studied flash sintering in tin dioxide with and without the addition of 2wt% MnO_2 as a sintering aid, using an initial electric field of 80V/cm with furnace temperatures of 900, 1100 and 1300ºC. Densification was minimal for the lower current limit of 1A, but increased when 5A current limit was used. For the pure SnO_2 samples, the primary microstructural process observed was grain welding, with the densities of samples remaining low at around 45% of the theoretical maximum density even after the heat treatment. It is questionable whether flash sintering has truly occurred in these samples. However for the samples with MnO_2 addition, samples reached up to 91.8% of the theoretical density and also maintained reduced grain sizes. These observations could be due to extensive Joule heating in the sample. While some densification is evident, this paper [94] presents limited evidence of flash sintering in these samples, and further work is required to establish the optimal flash sintering conditions for this material.

4.3.5 Zinc oxide

Like tin oxide, zinc oxide is an n-type semiconductor material and is used in varistors [11]. Schmerbauch *et al.* [40] showed that zinc oxide exhibits flash sintering for initial electric fields above 80V/cm, with onset furnace temperatures of 625ºC at 160V/cm and 675ºC for 80V/cm (151 A/mm^2 current limit). Samples reached bulk densities of around 94.5% of the theoretical maximum, with this densification almost exclusively occurring during the flash event during ramp-up, rather than during the later isothermal hold step. At lower electric fields field-assisted sintering processes were observed. In contrast two papers from the group of Luo at University of California San Diego (Zhang *et al.* [95] and Zhang and Luo [51]) used much higher electrical fields to flash sinter zinc oxide at temperatures as low as 108ºC (500V/cm, current density limit of 153 mA/mm^2) in a reducing atmosphere (Ar + 5mol% H_2). The density of these samples was 97.4%. Further increasing the electric field to

1000V/cm did not produce a significant increase in the density. The lower onset temperature is attributed to the fact that partially reduced ZnO has higher electrical conductivity compared to the stoichiometric material, enabling the flash event to occur at lower furnace temperatures. Notably, using the reducing atmosphere also eliminated the marked differences between the grain size observed between the anode and cathode regions of the samples in the earlier work (Zhang *et al.* [95]). This paper is unusual in using different atmospheres for the heat-treatments involved in flash sintering, and the findings indicate that this is a processing parameter which may well be expected to enhance flash sintering in other similar materials.

4.4 Materials for use in Solid Oxide Fuel Cells

Solid oxide fuel cells (SOFC) have huge potential for energy generation with low pollution [96]. However they necessarily consist of several materials, including metals and ceramics, which often have non-compatible optimal processing conditions [97]. This may lead to deleterious reaction layers at the interfaces between different materials. Flash sintering enables the reduction of furnace temperatures required to densify the ceramic materials and so better SOFCs could be produced. In addition, SOFCs generally operate at high temperatures >800°C due to the ionic conductivity of currently used materials [98]. If high densification could be achieved in materials with higher ionic conductivity at lower temperatures, the working temperature could be reduced.

Flash sintering has been studied in a number of materials used in SOFCs. Prette *et al.* [97] found that samples consisting of Co_2MnO_4, used as a protective shielding material for metal interconnects, flash sintered to full density at temperatures as low as 325°C in the fairly modest electric field of 12.5V/cm. This study did not however address how this technique might be practically applied to the SOFC interconnects, dealing only with a freestanding dogbone of Co_2MnO_4 rather than a Co_2MnO_4 coating on a metal interconnect, a combination which would be expected to change the current flow through the ceramic.

Several studies on the viability of flash sintering materials for solid electrolytes for SOFCs have been carried out. The protonic conductor gadolinium-doped barium cerate ($BaCe_{0.8}Gd_{0.2}O_{3-\delta}$) was flash sintered by Muccillo *et al.* [99] with the aim of reducing the temperature required to sinter to full density. Pulses of AC current were used to weld the grains at 910ºC with approximately 9V/cm electric field. A density of 84% of the theoretical density was reached, however this was found to be inhomogeneous within the sample, and further optimisation of the conditions is required. Rare earth-doped ceria or RE-DC of various compositions has been the subject of several flash sintering studies, as it has good properties for SOFCs which are hampered by high (1700-1800ºC) densification temperatures. Building on earlier work [48], Jiang *et al.* [96] showed that under 90V/cm and ~86mA/mm^2 current density, $Ce_{0.9}Gd_{0.1}O_{1.95}$, $Ce_{0.8}Gd_{0.2}O_{1.9}$ and $C_{0.8}Sm_{0.2}O_{1.9}$ flash sintered at furnace onset temperatures of 635ºC, 554ºC and 667ºC respectively, with corresponding densities of 93.7%, 94.7% and 99.8%. While these works used dry uniaxial-pressed samples with low levels of added binder, Akbari-Fakhrabadi *et al.* [42] used the commonly used method of tape casting, which required significantly higher levels of binder and dispersants, to construct the Gd-doped ceria electrolyte samples for flash sintering. Akbari-Fakhrabadi observed flash sintering in $Ce_{0.9}Gd_{0.1}O_{1.95}$ at 875ºC under electric field of 70V/cm, with a current limit of 0.5A (corresponding to a current density limit of approximately 0.4A/mm^2 calculated with the given sample dimensions before binder burnout) [42]. Scanning electron micrographs show that the samples were not fully dense (though the density is not stated) and had an inhomogenous microstructure, suggesting that the flash sintering conditions used here are not optimised [42]. Most recently, Biesuz *et al.* [98] studied the flash sintering of $Ce_{0.9}Gd_{0.1}O_{1.95}$ pellets with silver electrodes, and found flash sintering onset temperatures of 700ºC for 75V/cm and 550ºC for 150V/cm, with current density limited to around 55mA/mm^2. Given the different conditions used, these findings are in line with those of Jiang *et al.* [96] but somewhat lower temperatures than Akbari-Fakharbadi [42]. However in this case Biesuz *et al.* [98] found that their samples sintered to densities between 98-100% with grain sizes of 300-500nm, giving an electrolyte which is ideal for SOFC applications [98].

Lanthanum-based materials find applications in SOFCs as electrolyte and cathode materials. LSCF ($La_{0.6}Sr_{0.4}Co_{0.2}Fe_{0.8}O_3$) has suitable ionic conductivity for use as a cathode in SOFCs, and has been shown to flash sinter at furnace temperatures below 100ºC in the relatively low electric field of 7.5V/cm with 1.55A/mm^2, compared to 1300ºC for heat treatment under zero electric field [49]. The lowest recorded furnace temperature of 25ºC for flash sintering occurred for an electric field of 12.5V/cm. These extraordinarily low processing temperatures, lower than that of many polymers, is apparently due to the conductivity of the LSCF material, where the conductivity is enhanced by polaron hoping. LSGM ($La_{0.8}Sr_{0.2}Ga_{0.8}Mg_{0.2}O_{3-\delta}$) is proposed as an alternative electrolyte for SOFCs and flash sinters at 690ºC under 100V/cm and 67mA/mm^2 current density limit. However these conditions did not result in full densification of the samples, with the conditions above resulting in a sample of 88.5% density. It was established that increasing the current density to 120mA/mm^2 resulted in samples of 97.4% density.

Finally, some initial efforts at flash sintering composite materials have also been made for SOFC applications. Gaur and Sglavo [49] mixed composites of LSCF and GDC to investigate the effect on flash sintering. Ratios of LSCF:GDC content in the composites were 60:40, 50:50 and 20:60, as well as pure samples of LSCF and GDC. Flash sintering was observed for 40:60 composite at 10V/cm at 905ºC, whereas it occurs at 5V/cm and 210ºC for pure LSCF and at 30V/cm and 990ºC for pure GDC. It is established that the higher the LSCF content of the composite the lower the furnace temperature required, as might be expected. However in all cases the power dissipation is significantly higher for the composites than the pure materials. The findings indicate cooperative mechanisms occur between the more electrically conducting LSCF phase and the more resistive GDC phase.

Liu *et al* [100] sintered layered structures for SOFC applications containing YSZ films stacked on NiO anodes, with an $La_{0.8}Sr_{0.2}MnO_x$ cathode added on top. This cell was sintered at a relatively low voltage with the intention of using the electric field to enhance sintering rates and supress grain growth, rather than to obtain the rapid densification of flash sintering, and this was indeed achieved. Similarly Francis *et al.* [101] also sintered composite materials for SOFC applications, this time with

a complex structure of multiple pairs of anode-electrolyte layers consisting of a nickel oxide and zirconia anode and a cubic zirconia (8YSZ) electrolyte. Stacked tape-cast samples of these materials (in combination as well as anode-only and electrolyte-only) were assembled and flash sintered with platinum wire electrodes twisted around each end of the samples. At 150V/cm field (applied along the plane of the layers), flash sintering occurred at 750ºC for the sample consisting only of electrolyte material, 1005ºC for the anode sample, and 915ºC for the multilayer (which consisted of 50% electrolyte layers and 50% anode layers). In the multilayer sample, strong bonding between layers was observed with no delamination or obvious mixing between layers. However the flash sintering behaviour observed in Francis *et al.* [101] suggests some interaction between the layers of different materials is occurring during the flash process, making the behaviour of the multilayer sample different from that of the samples composed of one type of material only. As multi-layered, tailored-microstructure ceramics are useful for a wide range of applications, including enhanced mechanical properties [102–105] and electromagnetic devices [106,107], this is an area which is ripe for further investigation.

4.5 Ferroelectric Ceramics

Ferroelectric materials are self-polarising materials which find applications in energy storage, particularly as capacitor materials [3]. Three ferroelectric materials have so far been shown to undergo flash sintering; strontium titanate [108], barium titanate [35,109,110] and potassium niobate [111].

Strontium titanate was shown to flash sinter at 1200ºC onset furnace temperature in an initial electric field of 150V/cm at 500mA to greater than 95% of the theoretical maximum density with a grain size around 1μm [108]. In comparison conventional sintering at 1400ºC for 1h resulted in a 92% dense sample with grain size of 1.5μm. Studies of the sintered material by X-ray diffraction indicated some distortions in the structure, and high resolution transmission electron microscopy confirmed the presence of non-stoichiometric Ruddleson-Popper phases in the material [108]. These are likely to cause changes in the conductivity of the $SrTiO_3$. These defect states were observed in both

conventionally sintered and flash sintered samples though the concentrations were lower in the flash sintered samples. However, whether these defect phases are a cause or a result of different types of sintering behaviour has not been conclusively determined in this work. It is not clear from this study whether the defect states were thought to be present prior to the start of the sintering (formed before or during heating), and have therefore been *consumed* to a greater extent during flash sintering compared to conventional sintering, or if they were *created* during the sintering event and therefore more were produced, perhaps due to the longer time at high temperature, during the conventional sintering compared to flash sintering.

Barium titanate is another widely used ferroelectric material, with particular interest for supercapacitor materials due to its high dielectric permittivity. Flash sintering in barium titanate has been shown to occur for initial electric fields above 250V/cm for current density of 9.3mA/mm^2 by M'Peko *et al.* [109] and for current density of 25mA/mm^2 for 250V/cm by Uehashi *et al.* [110]. Under initial electric field of 1000V/cm the flash sintering onset furnace temperature reduced to as low as 612°C, compared to 1350°C for 1h for conventional sintering [109]. However it is noticeable that the final density of the barium titanate in these studies was reduced significantly for flash sintering compared to conventional sintering. A maximum density of 94.3% (250V/cm) compared to 96.4% for conventional sintering was observed by M'Peko *et al.* [109], while Ueshashi *et al.* [110] observed the even lower degree of densification of ~75% density for 250V/cm and ~60% for 350V/cm, presumably due to the higher current density. However, at between 0.6μm for 250V/cm and 0.3-0.4μm for 500V/cm the grain size in the flash sintered samples was significantly smaller than for conventional sintering (15μm after 1h) [109]. M'Peko *et al.* [109] also demonstrated that raising the current density limit too high can result in significant inhomogeneities in the microstructure, which is confirmed in a later study by Yoshida *et al.* [35] who examined damage in barium titanate polycrystalline ceramics exposed to electric fields of 133V/cm. Layers of second phase material with reduced barium content were found at the grain boundaries, suggesting that electric conduction through the grain boundaries may trigger the flash sintering event in barium titanate.

As described in Section 2.4 above, grain size usually increases with density so the need to find a suitable compromise between high density and small grain size is not unusual in ceramic processing. As barium titanate is a functional material it is not necessarily the case that full densification is required for optimised dielectric properties. The dielectric properties are strongly grain size dependent, with the best dielectric performance at 100kHz occurring for the flash sintered samples with 0.6μm grain size, albeit with a small decrease in the measured Curie temperature (temperature of transition to the cubic non-ferroelectric phase) of 128°C compared to 132°C for conventional sintering [109]. It should be noted however that all the papers discussed above use <100nm size barium titanate as the starting powder which are likely to be primarily composed of the cubic phase [112]. Starting with a larger particle size powder composed primarily of tetragonal phase barium titanate may improve the dielectric properties further for the lower temperature flash sintering processes.

Potassium niobate ceramic materials are lead-free ferroelectric materials developed to replace lead zirconium titanate. Potassium niobate is however very difficult to sinter to high density due to evaporation of potassium oxide above 800°C [111]. Flash sintering at lower furnace temperatures would therefore be expected to reduce the evaporation of the potassium oxide, and indeed at 600V/cm initial electric field and ~11mA/mm^2 current density maximum, the flash sintering onset temperature of $KNbO_3$ was just 750°C [111]. Samples of 95% density with stoichiometric composition were obtained [111]. A separate study examining flash sintering in the related material $Ka_{0.5}Na_{0.5}NbO_3$ required higher furnace temperatures for the onset of flash sintering of 990°C, which with initial electric field of 250V/cm and current density of 20mA/mm^2 gave samples of 94% of the theoretical density of the material [113]. A liquid phase forming at the grain boundary caused inhomogeneous microstructure, though this could be reversed by further heat treatment.

4.6 Magnetic Materials

Only one magnetic material has been flash-sintered to date. The flash spark plasma sintering route was used to fully densify Nd-Fe-Dy-Co-B-Ga powders with a short pre-heating step [114]. Importantly, anisotropic properties were attained in the flash spark plasma sintered samples, with greater anisotropy than for conventional SPS, and the retained nanoscale grain size contributed to a greater magnetic coercivity. This initial study demonstrates the viability of flash sintering for a wide range of ceramic materials, some of which, like this permanent magnet, have previously only been fully densified by the use of very high pressures.

4.7 Composite Materials

While the addition of small quantities of doping materials is relatively common in flash sintering studies, the flash sintering of composite materials containing large volume fractions of two or more phases is less widespread. By combining the properties of different ceramic materials, composites can possess superior mechanical and functional properties compared to monolithic ceramics [11]. For example, adding alumina to zirconia alters the grain boundary properties, giving finer grain sizes and therefore enhanced mechanical properties compared to the parent materials [12]. The reduced furnace temperatures required for flash sintering may enable new combinations of ceramic materials to be produced.

To date, studies of flash sintering of composite materials have primarily been carried out on materials containing yttria-stabilized zirconia. One exception to this is the study of flash sintering in alumina-titania composites by Jha *et al.* in two studies [115,116]. In the first study, large alumina particles within a fine titania matrix were shown to flash sinter at temperatures between 825°C and 850°C with electric field of 250V/cm and with a current density limit of 18mA/mm^{2}. With high volume fractions of alumina (19%) however the densification is limited to 90% of the theoretical maximum (calculated by a rule of mixtures basis as no phase changes are observed in X-ray diffraction), while samples with lower fractions of alumina sintered to nearly full density. In the later

work, 20vol.% alumina was added to titania powder with similar particle sizes and flash sintered at 830ºC, 500V/cm with a range of current density limits between ~20-40mA/mm^2 [115]. In this case a phase transformation is apparent for hold times after flash sintering of 150s or more. The authors attribute the differences in behaviour between the two studies to the differences in the size of the alumina particles used which alter the extent to which contstrained sintering [117] occurs.

Flash sintering behaviour has also been studied in zirconia-based materials with additions of alumina [118], silicon carbide whiskers [119], and yttrium aluminium garnet (YAG) with alumina [120]. Liu *et al.* [119] showed that the flash sintering of silicon carbide whiskers in a 3Y-TZP matrix resulted in a dense (>95%) microstructure under 120-140V/cm, 80mA/mm^2 and at 1000ºC. The process was carried out in air without significant oxidation of the silicon carbide whiskers. Alumina-3Y-TZP composites are commonly produced to optimise the toughness of the ceramic material. Bichaud *et al.* [118] showed that 3Y-TZP with up to 40% alumina added will flash sinter at 1100ºC with 200V/cm initial electric field, while a composite of 60% alumina in 3Y-TZP did not flash sinter at up to 1100ºC. The findings indicate that the samples conductivity is a critical factor in determining the onset time for flash sintering, with a threshold value above which flash sintering occurs immediately upon reaching the flash sintering onset furnace temperature. Therefore the composition of composite materials must be carefully managed to optimise the flash sintering conditions. Naik *et al.* [120] studied similar materials consisting of 50vol% 3Y-TZP-alumina composites, which flash sintered at 1060ºC under 150V/cm. Compared to pure 3Y-TZP, which will flash sinter at 850ºC and 120V/cm [20], and pure alumina, which will not flash sinter without doping under these conditions [87], it seems that the properties of the composite are clearly not entirely predictable from the parent materials in both studies. This suggests that in composite materials undergoing flash sintering some interaction between the defect states from the parent materials can affect the flash sintering process. This presents the intriguing possibility of creating composite ceramic materials with tailored optimised processing conditions, which may be useful to obtain processing compatibility for multimaterial artefacts.

The eutectic material Al_2O_3-$Y_3A_{l5}O_{12}$-ZrO_2, produced from a mixture of alumina, yttria and zirconia powders, is prized for its mechanical properties particularly at high temperatures [121]. Current processing methods are time-consuming directional solidification routes which are difficult to achieve in practice [122]. Flash sintering was used to densify the eutectic ceramic to 4.40g/cm^3 at 1345°C and 495V/cm, 0.3A [122]. The eutectic ceramic had high hardness and fracture strength [122], though it is likely that further optimisation of the flash sintering conditions in order to reach full density is necessary, given that the values well short of conventionally processed eutectic ceramic of the same composition.

5. Theories of the mechanism of flash sintering

While the rapid densification directly observed during flash sintering is now well established as a phenomenon, the mechanisms underlying the process are still the subject of fierce debate. In particular, the field is divided as to whether flash sintering can be entirely explained as a process of thermal runaway caused by Joule heating, or whether additional contributions to mass transport from defects such as Frenkel pairs is required to fully account for the rapid sintering rates to high degrees of densification observed in flash sintering. These factors are discussed in the following section and first summarising the observed behaviours associated with flash sintering, which theories to explain the occurrence in different materials must explain.

5.1 Experimentally-derived observations of the regimes of flash sintering behaviour

In the early flash sintering papers, the furnace temperature was ramped up while the sample was subjected to a set electric field value [20]. Flash sintering occurred spontaneously at an onset temperature of the furnace. There are clear problems with this approach, in that the true sample temperature is not known, and particularly at high heating rates the temperature of the sample could differ considerably from that in the furnace. As the expected parameters required became better established, it was easier for later experiments to introduce an isothermal hold in temperature at a

suitable level. Experiments carried out in this way established that flash sintering can also occur after an incubation time at a particular temperature [39]. In addition it has been established using measurements of the optical spectrum of the emission that the glowing of the samples during flash sintering is due to electroluminescence, rather than black body radiation [34,123]. The collective findings of these experiments [34,39,123] have led to the acknowledgement of the importance of current and sample conductivity in the flash sintering process in more recent papers.

In the introduction to their 2016 paper, Jha *et al.* [73] summarise the findings of earlier isothermal experiments with flash sintering of 3Y-TZP, describing three distinct stages of the process, specifically:

- Stage I: before the flash occurs but while at stable furnace temperature. Power supply is under voltage control and the sample heats by Joule heating. Duration: 1s-several hours.
- Stage II: The flash process, occurring at isothermal furnace temperature. The power supply is switched from voltage to current control and sintering occurs within 1-5s. Electroluminescence is observed. Grain growth may be observed.
- Stage III: Power supply is still under current control, and maintains the flash state within the sample. Sample is sintered, grain growth occurs rapidly, and electroluminescence is observed. The furnace can be turned off and the sample cooled during this stage.

The length of each stage depends on the material and the process conditions (electric field and furnace temperature). A complete theory of flash sintering needs to explain the mechanisms for the behaviour during each stage.

It should also be noted in considering the validity of proposed flash sintering theories that the switching of the power supply from voltage control to current control is an essential step in avoiding entering an uncontrollable state of electrical runaway which would eventually lead to the melting of the sample. By switching to current-control, the power becomes constant and the sample enters a steady state condition as the voltage and current are both stable.

5.2 Modelling flash sintering as Joule heating causing thermal runaway

Several researchers have presented models which determine that flash sintering behaviour can be entirely attributed to thermal runaway caused by Joule heating (heating under an Ohmic regime which occurs due to the resistance of the material, and which is proportional to the square of the current). Todd *et al.* [8] present a detailed analysis of experimental data used to inform a numerical model based on an inverse Arrhenius dependence of resistivity on temperature (a more detailed mathematical analysis is presented in the paper by Hewitt *et al.* [124] from the same research group). Using this model, Todd *et al.* [8] account for the incubation time for the onset of flash sintering under isothermal conditions, as well as the relationship between the furnace temperature at the onset of flash sintering and the applied electric field. In addition, a relationship between the furnace temperature and the electric field gives a critical condition for the onset of flash sintering with close agreement with experimental data for the case of thermally insulating electrodes [124].

A dynamic, non-uniform numerical model was also developed using Fortran to closely explore the effect of different parameters [8]. This determined that a high field in flash sintering, resulting in the lowest furnace temperatures, may cause non-uniform increases in temperature and hence cracking during the process [8]. This has particularly important implications for the scale-up of flash sintering. The current is identified as a key criterion for successful sintering due to its influence on the specimen temperature, though care must be taken to avoid locally high currents which will lead to inhomogeneous temperature distribution in the sample [8].

A simpler expression for the relationship between the onset temperature and the electric field was determined by Dong and Chen [125] by considering the contributions of Joule heating, radiative heating from the furnace, and radiative cooling from the insulator to the environment. According to their analysis, the electric field (E) and onset furnace temperature (T_F) are related as shown in Equation (1):

$$\ln\left(\frac{E^2}{T_F^4}\right) = \frac{E_a}{k_B T_F} + \ln\left(\frac{\varepsilon\sigma S d^2 R_0}{\beta}\right) \quad (1)$$

where E_a is the activation energy for the temperature dependent resistance while R_0 is the pre-exponential factor in this relationship, k_B is the Boltzmann constant, ε is the emissivity, S is the surface area of the sample, σ is the Stefan-Boltzmann constant, d is the sample length, and β is a numerical constant. Fitting experimental data from the literature to this equation gives a map of processing conditions for electronic semiconductors, oxygen ion conductors and insulating oxides [125]. To further verify the accuracy of this analysis, which currently includes several outliers, more experimental data should be generated.

Finally, Zhang *et al.* also analysed thermal runaway during flash sintering using experimental data for zinc oxide, with the key condition for thermal runaway occurring when more heat is generated than can be dissipated as in Equation 2 for conditions of $T = T_F$:

$$\frac{d\sigma}{dT} > \frac{\alpha}{E^2 V_s} \qquad (2)$$

where $d\sigma/dT$ is the rate of rate of change of electrical conductivity with temperature, evaluated here at the onset furnace temperature for flash sintering, α is a parameter calculated from the increase of heat transfer rate with increasing sample temperature, E is the applied electric field, and V_s is the volume of the sample. This model presents a balance between the material dependent properties (left hand side of Equation 2) and the experimental design variables such as the sample geometry and the electric field (right hand side) [95].

Jha *et al.* state that Joule heating causing thermal runaway is insufficient to fully explain the flash sintering process, arguing that linearization of parameters during the numerical analysis which accounts for thermal runaway is unlikely to be valid for a non-linear phenomenon such as the increases in sample conductivity seen in flash sintering [73]. However it should be noted that a recent analysis by Pereira da Silva *et al.* uses a non-linear approach but also concludes that the critical condition for flash sintering can be determined from thermal runaway rather than being defect mediated [126], a clear contradiction in findings which is not yet resolved.

5.3 Modelling flash sintering as defect avalanches causing increases in diffusion at grain boundaries

The argument that thermal runaway alone cannot account for the densification rates in flash sintering requires that at least one other mechanism acts to accommodate the observed phenomenon. This is generally held to be mediated by a colossal defect population which forms and diffuses during the flash sintering process.

In papers drawing on long-standing research interests in the effect of electric field on ceramic materials, Narayan argues that the interaction between cation and anion vacancies with the elastic and electronic fields increases the diffusion rates along dislocations and grain boundaries within the sintering material [127,128]. This mechanism leads to retarded grain growth at low electric fields (as observed by Yang and Conrad [7] and by Ghosh *et al.* [70]) and to Joule heating at higher fields because the concentrations of defects are much higher. At the highest fields an avalanche effect occurs, as grain boundaries are locally heated to melting temperatures. Narayan attributes flash sintering to the high diffusivity of defects at the grain boundaries which are at high (liquid) temperatures, enabling densification during seconds [127]. Grain growth is therefore retarded during the flash sintering because of the grain boundary melting [128]. However, this model does explicitly require that flash sintering occurs in the liquid state, stating that the diffusivities of the materials is not high enough to account for the observed sintering rates in the solid state. It might be expected that some evidence on the grain boundaries would be detectable if this were the case.

Rishi Raj and co-workers [20,34,37,39,73,129] likewise attribute the effect of flash sintering to a combination of Joule heating from power dissipation and the contribution of these defect-mediated processes, with different mechanisms occurring in different stages of the flash sintering process, and have explicitly stated that Joule heating alone cannot completely account for the flash sintering mechanism [130]. However they do not agree that the temperatures rise sufficiently in the sample to enable the molten grain boundary mechanism proposed [73]. These defects are thought to aid chemical diffusion, and also cause electroluminescence and non-equilibrium phase transformations observed for flash sintering of 3Y-TZP particularly during Stage III of the process

where Joule heating considerations no longer apply [73]. At the furnace temperature, it has been suggested that the nucleation of regions of high defect concentration occurs, enhancing both diffusivity (neutral defects) and conductivity (electron-hole pairs) which coalesce to larger and larger regions of high permittivity [130]. This mechanism has been proposed as the initiator of the later observed Joule heating in the sample.

5.4 Insight from the behaviour of composite materials

In Section 4.7 it was noted that the behaviour of composite material under flash sintering conditions does not seem to follow a straightforward relationship based on the relative volume fractions of the parent phases. The behaviour of composite materials undergoing flash sintering has not yet been explained by the theories presented in the literature, in particular the constrained sintering observed for titania with large alumina particles contained in the matrix [115] and in multilayer anode/electrode structures designed for solid oxide fuel cells [101]. The interaction between different phases despite the lack of inter-diffusion evident in the layered structure using electron microscopy suggests that an interaction of defects between the two phases must occur in order to account for the flash sintering conditions required, strengthening the argument that defect populations contribute to flash sintering behavoiur. In addition the mechanism by which sintering additives change the flash sintering behaviour in materials such as alumina are not fully established [87,88]. The role of defects in mediating flash sintering remains an open question, and interesting insights may be obtained from experiments using different types of composite material structures.

5.5 Summary of proposed theories of flash sintering

It is clear from the reports discussed in the sections above that researchers in the field are far from agreement as to the explanation for the mechanism of flash sintering in ceramic materials. While Joule heating has been shown numerically to account for the thermal runaway observed at the initiation of the flash event [8,95,125], Raj and co-workers argue that there are a number of other

factors, including observed electroluminescence, phase transitions, and chemical diffusion, which are observed in experiments on flash sintering and cannot be due to the Joule heating process [73]. The argument that the process is mediated by defects at grain boundaries reaching liquid temperatures [127,128] is not verified by experimental study [130], though defects do play a role in the densification and grain modification given the different diffusion behaviours observed under DC and AC current [41] and the behaviour observed in composite and doped materials [87,88,101,115]. It is necessary to obtain more reliable data for further insight into the various stages of the flash sintering process, and the mechanisms occurring under those conditions. In particular, an understanding of the complex interplay between material factors (material composition, including small impurity content, grain size and distribution) and the flash sintering parameters (voltage, electric field, current density, furnace temperature, electrode type, and pressure applied), which have been identified in this review, is necessary to attain a sufficient understanding of the flash sintering process such that the conditions may be predicted systematically for a wide range of ceramic materials, both monolithic and composite.

6. Conclusions

This review has detailed the work carried out to date on the flash sintering process in ceramic materials whereby under high electric fields and at elevated furnace temperature a range of ceramic materials are observed to sinter rapidly to high density. Variations in experimental apparatus, specimen geometry, and the electrode material and method of electrode attachment are apparent throughout the literature. At this relatively early stage in the research in this field, it is perhaps unsurprising that the effect of these variations has not been systematically examined; studies where such factors have been investigated, such as varying the electrode material [44], have indicated interesting effects on the processing requirements for flash sintering for the same ceramic material (alumina) which should be investigated further.

Flash sintering, along with other electric-field assisted densification processes, enables a greater degree of control over ceramic processing than can be achieved by conventional processing techniques. The option to flash sinter free-standing samples lessens the constraints on sample shape, at least for small artefacts, typical to die-mediated pressure-assisted methods such as spark plasma sintering and hot pressing. Flash sintering therefore represents a powerful addition to the previous arsenal of ceramic processing methods. However while significant experimental work has enabled a better (though incomplete) understanding of the conditions necessary for flash sintering, the mechanisms underlying flash sintering are not yet firmly established for any material. It is clear from the above discussion that a universal theory for the mechanism of flash sintering has not yet been accepted by the research community, with different proposals for Joule heating and defect mediated mechanisms being justified by various analyses of the available experimental data. One route to resolving the current situation is to obtain more comparative experimental data for different materials under the same conditions of current density limit, furnace temperature, and electric field. Further research using comparable experimental apparatus, materials with carefully controlled purity and particle size, and with the *in situ* monitoring of material properties during the flash process is required. In addition, interesting insights into the origin of the flash sintering mechanisms can be gained from studies on different combinations and constructions of composite materials, the investigation of which is so far extremely limited. However, with a greater understanding of the processing conditions required to induce flash sintering, the technique could be used to produce ceramic materials with tailored microstructures and unique geometries which may realise new applications [40].

References

[1] R.H.R. Castro, K. van Benthem, eds., Sintering, 1st ed., Springer-Verlag, Berlin Heidelberg, 2013.

[2] T. Kumagai, Rapid Densification of Yttria-Stabilized Tetragonal Zirconia by Electric Current-Activated/Assisted Sintering Technique, J. Am. Ceram. Soc. 94 (2011) 1215–1223. doi:10.1111/j.1551-2916.2010.04235.x.

[3] C.B. Carter, M.G. Norton, Ceramic Materials: Science and Engineering, 2nd ed., Springer, London, UK, 2013.

[4] M. Cologna, A.L.G. Prette, R. Raj, Flash-Sintering of Cubic Yttria-Stabilized Zirconia at 750°C for Possible Use in SOFC Manufacturing, J. Am. Ceram. Soc. 94 (2011) 316–319. doi:10.1111/j.1551-2916.2010.04267.x.

[5] D. Yang, R. Raj, H. Conrad, Enhanced Sintering Rate of Zirconia (3Y-TZP) Through the Effect of a Weak dc Electric Field on Grain Growth, J. Am. Ceram. Soc. 93 (2010) 2935–2937. doi:10.1111/j.1551-2916.2010.03905.x.

[6] H. Conrad, D. Yang, Influence of an applied dc electric field on the plastic deformation kinetics of oxide ceramics, Philos. Mag. 90 (2010) 1141–1157. doi:10.1080/14786430903304137.

[7] D. Yang, H. Conrad, Enhanced sintering rate of zirconia (3Y-TZP) by application of a small AC electric field, Scr. Mater. 63 (2010) 328–331. doi:10.1016/j.scriptamat.2010.04.030.

[8] R.I. Todd, E. Zapata-Solvas, R.S. Bonilla, T. Sneddon, P.R. Wilshaw, Electrical characteristics of flash sintering: thermal runaway of Joule heating, J. Eur. Ceram. Soc. 35 (2015) 1865–1877. doi:10.1016/j.jeurceramsoc.2014.12.022.

[9] F. Liu, M. Gong, Nano-Scaled Grain Growth, in: R.H.R. Castro, K. van Benthem (Eds.), Sintering, 1st ed., Springer-Verlag, Berlin Heidelberg, 2013: pp. 35–55.

[10] Lucideon, Field Enhanced Sintering, (2016). http://www.lucideon.com/industries/ceramics/field-enhanced-processing (accessed May 30, 2016).

[11] Y. Chiang, D.P. Birnie (III), W.D. Kingery, Physical Ceramics: Principles for Ceramic Science

and Engineering, 1st ed., John Wiley & Sons Ltd, 1997.

[12] F.L. Riley, Structural Ceramics: Fundamentals and Case Studies, 1st ed., Cambridge University Press, Cambridge, UK, 2009.

[13] D. Garcia, A. Klein, D. Hotza, Advanced ceramics with dense and fine-grained microstructures through fast firing, Rev. Adv. Mater. Sci. 30 (2012) 273–281. http://www.ipme.ru/e-journals/RAMS/no_33012/07_garcia.pdf (accessed September 19, 2014).

[14] R.H.R. Castro, Overview of Conventional Sintering, in: R.H.R. Castro, K. van Benthem (Eds.), Sintering, 1st ed., Springer-Verlag, Berlin Heidelberg, 2013: pp. 1–16.

[15] R. V Brook, R. Cahn, P. Haasen, E.S. Kramer, eds., Materials Science and Technology: Vol. 17B Processing of Ceramics (Part II), 1st ed., VCH Publishers Inc, New York, 1996.

[16] R.L. Coble, Sintering crystalline solids. I. intermediate and final state diffusion models, J. Appl. Phys. 32 (1961) 787–792. doi:10.1063/1.1736107.

[17] R.L. Coble, Sintering crystalline solids. II. experimental test of diffusion models in powder compacts, J. Appl. Phys. 32 (1961) 793–799. doi:10.1063/1.1736108.

[18] J. Reed, Principles of Ceramic Processing, 2nd ed., Wiley-Interscience, New York, USA, 1995.

[19] S.J. Dillon, M.P. Harmer, G.S. Rohrer, The Relative Energies of Normally and Abnormally Growing Grain Boundaries in Alumina Displaying Different Complexions, J. Am. Ceram. Soc. 93 (2010) 1796–1802. doi:10.1111/j.1551-2916.2010.03642.x.

[20] M. Cologna, B. Rashkova, R. Raj, Flash sintering of nanograin zirconia in <5 s at 850°C, J. Am. Ceram. Soc. 93 (2010) 3556–3559. doi:10.1111/j.1551-2916.2010.04089.x.

[21] J.A. Downs, V.M. Sglavo, Electric Field Assisted Sintering of Cubic Zirconia at 390°C, J. Am. Ceram. Soc. 96 (2013) 1342–1344. doi:10.1111/jace.12281.

[22] H. Conrad, D. Yang, Effect of the strength of an AC electric field compared to DC on the sintering rate and related grain size of zirconia (3Y-TZP), Mater. Sci. Eng. A. 559 (2013) 591–594. doi:10.1016/j.msea.2012.08.146.

[23] J.-M. Lebrun, T.G. Morrissey, J.S.C. Francis, K.C. Seymour, W.M. Kriven, R. Raj, Emergence and Extinction of a New Phase During On-Off Experiments Related to Flash Sintering of 3YSZ, J. Am. Ceram. Soc. 98 (2015) 1493–1497. doi:10.1111/jace.13476.

[24] R. Muccillo, M. Kleitz, E.N.S. Muccillo, Flash grain welding in yttria stabilized zirconia, J. Eur. Ceram. Soc. 31 (2011) 1517–1521. doi:10.1016/j.jeurceramsoc.2011.02.030.

[25] R. Baraki, S. Schwarz, O. Guillon, Effect of Electrical Field/Current on Sintering of Fully Stabilized Zirconia, J. Am. Ceram. Soc. 95 (2012) 75–78. doi:10.1111/j.1551-2916.2011.04980.x.

[26] L.B. Caliman, E. Bichaud, P. Soudant, D. Gouvea, M.C. Steil, A simple flash sintering setup under applied mechanical stress and controlled atmosphere, MethodsX. 2 (2015) 392–398. doi:10.1016/j.mex.2015.10.004.

[27] S. Grasso, T. Saunders, H. Porwal, O. Cedillos-Barraza, D.D. Jayaseelan, W.E. Lee, et al., Flash Spark Plasma Sintering (FSPS) of Pure ZrB2, J. Am. Ceram. Soc. 97 (2014) 2405–2408. doi:10.1111/jace.13109.

[28] S. Grasso, T. Saunders, H. Porwal, B. Milsom, A. Tudball, M. Reece, Flash Spark Plasma Sintering (FSPS) of α and β SiC, J. Am. Ceram. Soc. 99 (2016) 1534–1543. doi:10.1111/jace.14158.

[29] B. Niu, F. Zhang, J. Zhang, W. Ji, W. Wang, Z. Fu, Ultra-fast densification of boron carbide by flash spark plasma sintering, Scr. Mater. 116 (2016) 127–130. doi:10.1016/j.scriptamat.2016.02.012.

[30] S. Grasso, E.-Y. Kim, T. Saunders, M. Yu, A. Tudball, S.-H. Choi, et al., Ultra-Rapid Crystal Growth of Textured SiC Using Flash Spark Plasma Sintering Route, Cryst. Growth Des. 16

(2016) 2317–2321. doi:10.1021/acs.cgd.6b00099.

[31] O. Vasylkiv, H. Borodianska, Y. Sakka, D. Demirskyi, Flash spark plasma sintering of ultrafine yttria-stabilized zirconia ceramics, Scr. Mater. 121 (2016) 32–36. doi:10.1016/j.scriptamat.2016.04.031.

[32] E. Zapata-Solvas, S. Bonilla, P.R. Wilshaw, R.I. Todd, Preliminary investigation of flash sintering of SiC, J. Eur. Ceram. Soc. 33 (2013) 2811–2816. doi:10.1016/j.jeurceramsoc.2013.04.023.

[33] E. Zapata-Solvas, D. Gómez-García, A. Domínguez-Rodríguez, R.I. Todd, Ultra-fast and energy-efficient sintering of ceramics by electric current concentration, Sci. Rep. 5 (2015) 8513. doi:10.1038/srep08513.

[34] J.-M. Lebrun, R. Raj, A First Report of Photoemission in Experiments Related to Flash Sintering, J. Am. Ceram. Soc. 97 (2014) 2427–2430. doi:10.1111/jace.13130.

[35] H. Yoshida, A. Uehashi, T. Tokunaga, S. Jatsuhiro, T. Yamamoto, Formation of grain boundary second phase in BaTiO 3 polycrystal under a high DC electric field at elevated temperatures, J. Ceram. Soc. Japan. 124 (2016) 388–392. doi:10.2109/jcersj2.15259.

[36] M. Cologna, R. Raj, Surface Diffusion-Controlled Neck Growth Kinetics in Early Stage Sintering of Zirconia, with and without Applied DC Electrical Field, J. Am. Ceram. Soc. 94 (2011) 391–395. doi:10.1111/j.1551-2916.2010.04088.x.

[37] J.S.C. Francis, R. Raj, Flash-Sinterforging of Nanograin Zirconia: Field Assisted Sintering and Superplasticity, J. Am. Ceram. Soc. 95 (2012) 138–146. doi:10.1111/j.1551-2916.2011.04855.x.

[38] R. Muccillo, E.N.S. Muccillo, An experimental setup for shrinkage evaluation during electric field-assisted flash sintering: Application to yttria-stabilized zirconia, J. Eur. Ceram. Soc. 33 (2013) 515–520. doi:10.1016/j.jeurceramsoc.2012.09.020.

[39] J.S.C. Francis, R. Raj, Influence of the Field and the Current Limit on Flash Sintering at

Isothermal Furnace Temperatures, J. Am. Ceram. Soc. 96 (2013) 2754–2758. doi:10.1111/jace.12472.

[40] C. Schmerbauch, J. Gonzalez-Julian, R. Röder, C. Ronning, O. Guillon, Flash sintering of nanocrystalline zinc oxide and its influence on microstructure and defect formation, J. Am. Ceram. Soc. 97 (2014) 1728–1735. doi:10.1111/jace.12972.

[41] W. Qin, H. Majidi, J. Yun, K. van Benthem, Electrode Effects on Microstructure Formation During FLASH Sintering of Yttrium-Stabilized Zirconia, J. Am. Ceram. Soc. 99 (2016) 2253–2259. doi:10.1111/jace.14234.

[42] A. Akbari-Fakhrabadi, R.V. Mangalaraja, F.A. Sanhueza, R.E. Avila, S. Ananthakumar, S.H. Chan, Nanostructured Gd–CeO2 electrolyte for solid oxide fuel cell by aqueous tape casting, J. Power Sources. 218 (2012) 307–312. doi:10.1016/j.jpowsour.2012.07.005.

[43] L.B. Caliman, R. Bouchet, D. Gouvea, P. Soudant, M.C. Steil, Flash sintering of ionic conductors: The need of a reversible electrochemical reaction, J. Eur. Ceram. Soc. 36 (2015) 1253–1260. doi:10.1016/j.jeurceramsoc.2015.12.005.

[44] M. Biesuz, V.M. Sglavo, Flash sintering of alumina: Effect of different operating conditions on densification, J. Eur. Ceram. Soc. 36 (2016) 2535–2542. doi:10.1016/j.jeurceramsoc.2016.03.021.

[45] J. Gonzalez-Julian, K. Jähnert, K. Speer, L. Liu, J. Räthel, M. Knapp, et al., Effect of Internal Current Flow during the Sintering of Zirconium Diboride by Field Assisted Sintering Technology, J. Am. Ceram. Soc. 99 (2016) 35–42. doi:10.1111/jace.13931.

[46] S.K. Jha, J.M. Lebrun, K.C. Seymour, W.M. Kriven, R. Raj, Electric field induced texture in titania during experiments related to flash sintering, J. Eur. Ceram. Soc. 36 (2016) 257–261. doi:10.1016/j.jeurceramsoc.2015.09.002.

[47] Y. Du, A.J. Stevenson, D. Vernat, M. Diaz, D. Marinha, Estimating Joule heating and ionic conductivity during flash sintering of 8YSZ, J. Eur. Ceram. Soc. 36 (2015) 749–759.

doi:10.1016/j.jeurceramsoc.2015.10.037.

[48] X. Hao, Y. Liu, Z. Wang, J. Qiao, K. Sun, A novel sintering method to obtain fully dense gadolinia doped ceria by applying a direct current, J. Power Sources. 210 (2012) 86–91. doi:10.1016/j.jpowsour.2012.03.006.

[49] A. Gaur, V.M. Sglavo, Flash Sintering of (La, Sr)(Co, Fe)O 3 -Gd-Doped CeO 2 Composite, J. Am. Ceram. Soc. 98 (2015) 1747–1752. doi:10.1111/jace.13532.

[50] A. Gaur, V.M. Sglavo, Densification of La0.6Sr0.4Co0.2Fe0.8O3 ceramic by flash sintering at temperature less than 100 °C, J. Mater. Sci. 49 (2014) 6321–6332. doi:10.1007/s10853-014-8357-2.

[51] Y. Zhang, J. Luo, Promoting the flash sintering of ZnO in reduced atmospheres to achieve nearly full densities at furnace temperatures of <120°C, Scr. Mater. 106 (2015) 26–29. doi:10.1016/j.scriptamat.2015.04.027.

[52] T. Saunders, S. Grasso, M.J. Reece, Ultrafast-Contactless Flash Sintering using Plasma Electrodes, Sci. Rep. 6 (2016) 27222. doi:10.1038/srep27222.

[53] Lucideon, Field Enhanced Sintering Technology, Stoke-on-Trent, UK, 2016. http://www.lucideon.com/industries/ceramics/field-enhanced-processing.

[54] Lucideon, Low Energy Firing: The Story So Far, Stoke-on-Trent, UK, 2016. http://www.lucideon.com/materials-technologies/energy-reducing-firing-technology/the-technology.

[55] F. Trombin, R. Raj, Developing processing maps for implementing flash sintering into manufacture of whiteware ceramics, Am. Ceram. Soc. Bull. 93 (2014) 32–35.

[56] Lucideon, Field Enhanced Sintering - Tileware Applications, (2016). http://www.lucideon.com/materials-technologies/energy-reducing-firing-technology/tileware-applications (accessed May 30, 2016).

[57] Kennametal Manufacturing Ltd, Kennametal Newport Hosts Ribbon Cutting Ceremony for Grand Opening of Spark Plasma Sintering (SPS) Furnace, (2013). http://www.kennametal.com/en/about-us/news/spark-plasma-sintering-furnace-opens-in-uk.html (accessed May 30, 2016).

[58] K.I. Rybakov, E. a. Olevsky, E. V. Krikun, Microwave Sintering: Fundamentals and Modeling, J. Am. Ceram. Soc. 96 (2013) 1003–1020. doi:10.1111/jace.12278.

[59] Y. V. Bykov, K.I. Rybakov, V.E. Semenov, Microwave sintering of nanostructured ceramic materials, Nanotechnologies Russ. 6 (2011) 647–661. doi:10.1134/S1995078011050053.

[60] R.R. Thridandapani, D.C. Folz, D.E. Clark, Effect of electric field (2.45GHz) on sintering behavior of fully stabilized zirconia, J. Eur. Ceram. Soc. 35 (2015) 2145–2152. doi:10.1016/j.jeurceramsoc.2015.01.004.

[61] R. Raj, M. Cologna, J.S.C. Francis, Influence of Externally Imposed and Internally Generated Electrical Fields on Grain Growth, Diffusional Creep, Sintering and Related Phenomena in Ceramics, J. Am. Ceram. Soc. 94 (2011) 1941–1965. doi:10.1111/j.1551-2916.2011.04652.x.

[62] Y. V. Bykov, S. V. Egorov, A.G. Eremeev, V. V. Kholoptsev, K.I. Rybakov, A.A. Sorokin, Flash Microwave Sintering of Transparent Yb:(LaY) 2 O 3 Ceramics, J. Am. Ceram. Soc. 98 (2015) 3518–3524. doi:10.1111/jace.13809.

[63] Z. a. Munir, D. V. Quach, M. Ohyanagi, Electric Current Activation of Sintering: A Review of the Pulsed Electric Current Sintering Process, J. Am. Ceram. Soc. 94 (2011) 1–19. doi:10.1111/j.1551-2916.2010.04210.x.

[64] M. Tokita, Mechanism of Spark Plasma Sintering, in: Proceeding NEDO Int. Symp. Funct. Graded Mater., Japan, 1999: pp. 1–13. doi:10.1063/1.3622584.

[65] D.M. Hulbert, A. Anders, D. V. Dudina, J. Andersson, D. Jiang, C. Unuvar, et al., The absence of plasma in “spark plasma sintering,” J. Appl. Phys. 104 (2008) 033305. doi:10.1063/1.2963701.

[66] O. Guillon, Effect of Applied Stress and Heating Rate in Field Assisted Sintering, in: R.H.R. Castro, K. van Benthem (Eds.), Sintering, 1st ed., Springer-Verlag, Berlin Heidelberg, 2013: pp. 195–213. doi:10.1007/978-3-642-31009-6_9.

[67] T. Misawa, N. Shikatani, Y. Kawakami, T. Enjoji, Y. Ohtsu, H. Fujita, Observation of internal pulsed current flow through the ZnO specimen in the spark plasma sintering method, J. Mater. Sci. 44 (2009) 1641–1651. doi:10.1007/s10853-008-2906-5.

[68] U. Anselmi-Tamburini, G. Spinolo, F. Maglia, I. Tredici, T.B. Holland, A.K. Mukherjee, Field Assisted Sintering Mechanisms, in: R.H. Castro, K. van Benthem (Eds.), Sintering, 1st ed., Springer-Verlag, Berlin Heidelberg, 2013: pp. 159–193. doi:10.1007/978-3-642-31009-6_8.

[69] J. Langer, D. V. Quach, J.R. Groza, O. Guillon, A Comparison Between FAST and SPS Apparatuses Based on the Sintering of Oxide Ceramics, Int. J. Appl. Ceram. Technol. 8 (2011) 1459–1467. doi:10.1111/j.1744-7402.2010.02604.x.

[70] S. Ghosh, A.H. Chokshi, P. Lee, R. Raj, A Huge Effect of Weak dc Electrical Fields on Grain Growth in Zirconia, J. Am. Ceram. Soc. 92 (2009) 1856–1859. doi:10.1111/j.1551-2916.2009.03102.x.

[71] J.-C. M'Peko, J.S.C. Francis, R. Raj, Impedance Spectroscopy and Dielectric Properties of Flash Versus Conventionally Sintered Yttria-Doped Zirconia Electroceramics Viewed at the Microstructural Level, J. Am. Ceram. Soc. 96 (2013) 3760–3767. doi:10.1111/jace.12567.

[72] J.S.C. Francis, M. Cologna, R. Raj, Particle size effects in flash sintering, J. Eur. Ceram. Soc. 32 (2012) 3129–3136. doi:10.1016/j.jeurceramsoc.2012.04.028.

[73] S.K. Jha, K. Terauds, J. Lebrun, R. Raj, Beyond flash sintering in 3 mol % yttria stabilized zirconia, J. Ceram. Soc. Japan. 124 (2016) 283–288. doi:10.2109/jcersj2.15248.

[74] H. Braun, P. Herger, On the Separation of the Contributions of Powder Particle Cores and Intergranular Contacts to the Electric Resistivity of Compressed Powder Materials, Mater. Chem. 7 (1982) 787–802. doi:10.1017/CBO9781107415324.004.

[75] J.P. Kelly, O.A. Graeve, Effect of Powder Characteristics on Nanosintering, in: R.H. Castro, K. van Benthem (Eds.), Sintering, 1st ed., Springer-Verlag, Berlin Heidelberg, 2013: pp. 57–95. doi:10.1007/978-3-642-31009-6_4.

[76] S. Grasso, Y. Sakka, N. Rendtorff, C. Hu, G. Maizza, H. Borodianska, et al., Modeling of the temperature distribution of flash sintered zirconia, J. Ceram. Soc. Japan. 119 (2011) 144–146.

[77] H. Conrad, Space Charge and Grain Boundary Energy in Zirconia (3Y-TZP), J. Am. Ceram. Soc. 94 (2011) 3641–3642. doi:10.1111/j.1551-2916.2011.04823.x.

[78] R. Muccillo, E.N.S. Muccillo, Shrinkage control of yttria-stabilized zirconia during ac electric field-assisted sintering, J. Eur. Ceram. Soc. 34 (2014) 3871–3877. doi:10.1016/j.jeurceramsoc.2014.04.046.

[79] M. Cesar Steil, D. Marinha, Y. Aman, J.R.C. Gomes, M. Kleitz, From conventional ac flash-sintering of YSZ to hyper-flash and double flash, J. Eur. Ceram. Soc. 33 (2013) 2093–2101. doi:10.1016/j.jeurceramsoc.2013.03.019.

[80] S.-W. Kim, S.G. Kim, J.-I. Jung, S.-J.L. Kang, I.-W. Chen, Enhanced Grain Boundary Mobility in Yttria-Stabilized Cubic Zirconia under an Electric Current, J. Am. Ceram. Soc. 94 (2011) 4231–4238. doi:10.1111/j.1551-2916.2011.04800.x.

[81] M. Mashhadi, E. Taheri-Nassaj, V.M. Sglavo, Pressureless sintering of boron carbide, Ceram. Int. 36 (2010) 151–159. doi:10.1016/j.ceramint.2009.07.034.

[82] W. Ji, S.S. Rehman, W. Wang, H. Wang, Y. Wang, J. Zhang, et al., Sintering boron carbide ceramics without grain growth by plastic deformation as the dominant densification mechanism., Sci. Rep. 5 (2015) 15827. doi:10.1038/srep15827.

[83] X. Du, Z. Zhang, Y. Wang, J. Wang, W. Wang, H. Wang, et al., Hot-pressing kinetics and densification mechanisms of boron carbide, J. Am. Ceram. Soc. 98 (2015) 1400–1406. doi:10.1111/jace.13483.

[84] J.M. Lonergan, W.G. Fahrenholtz, G.E. Hilmas, Sintering Mechanisms and Kinetics for

Reaction Hot-Pressed ZrB_2, J. Am. Ceram. Soc. 98 (2015) 2344–2351. doi:10.1111/jace.13544.

[85] E. Zapata-Solvas, D.D. Jayaseelan, H.T. Lin, P. Brown, W.E. Lee, Mechanical properties of ZrB2- and HfB2-based ultra-high temperature ceramics fabricated by spark plasma sintering, J. Eur. Ceram. Soc. 33 (2013) 1373–1386. doi:10.1016/j.jeurceramsoc.2012.12.009.

[86] H. Yoshida, Y. Sakka, T. Yamamoto, J.-M. Lebrun, R. Raj, Densification behaviour and microstructural development in undoped yttria prepared by flash-sintering, J. Eur. Ceram. Soc. 34 (2014) 991–1000. doi:10.1016/j.jeurceramsoc.2013.10.031.

[87] M. Cologna, J.S.C. Francis, R. Raj, Field assisted and flash sintering of alumina and its relationship to conductivity and MgO-doping, J. Eur. Ceram. Soc. 31 (2011) 2827–2837. doi:10.1016/j.jeurceramsoc.2011.07.004.

[88] J. Gonzalez-Julian, O. Guillon, Effect of Electric Field/Current on Liquid Phase Sintering, J. Am. Ceram. Soc. 98 (2015) 2018–2027. doi:10.1111/jace.13571.

[89] S.K. Jha, R. Raj, The Effect of Electric Field on Sintering and Electrical Conductivity of Titania, J. Am. Ceram. Soc. 97 (2014) 527–534. doi:10.1111/jace.12682.

[90] Y. Zhang, J. Nie, J. Luo, Preface, J. Ceram. Soc. Japan. 124 (2016) 296–300. doi:10.2109/jcersj2.124.P4-1.

[91] J.M. Knaup, J. Marx, T. Frauenheim, Reduction of the TiO 2- x melting temperature induced by oxygen deficiency with implications on experimental data accuracy and structural transition processes, Phys. Status Solidi - Rapid Res. Lett. 8 (2014) 549–553. doi:10.1002/pssr.201409042.

[92] M.A. Ponce, C. Malagu, M.C. Carotta, G. Martinelli, C.M. Aldao, Gas indiffusion contribution to impedance in tin oxide thick films, J. Appl. Phys. 104 (2008). doi:10.1063/1.2975216.

[93] N. Dolet, J.M. Heintz, L. Rabardel, M. Onillon, P. Bonnet, Sintering mechanisms of 0.99SnO2-0.01CuO mixtures, J. Mater. Sci. 30 (1995) 365–368.

[94] R. Muccillo, E.N.S. Muccillo, Electric field-assisted flash sintering of tin dioxide, J. Eur. Ceram. Soc. 34 (2014) 915–923. doi:10.1016/j.jeurceramsoc.2013.09.017.

[95] Y. Zhang, J. Il Jung, J. Luo, Thermal runaway, flash sintering and asymmetrical microstructural development of ZnO and ZnO-Bi<inf>2</inf>O<inf>3</inf> under direct currents, Acta Mater. 94 (2015) 87–100. doi:10.1016/j.actamat.2015.04.018.

[96] T. Jiang, Z. Wang, J. Zhang, X. Hao, D. Rooney, Y. Liu, et al., Understanding the Flash Sintering of Rare-Earth-Doped Ceria for Solid Oxide Fuel Cell, J. Am. Ceram. Soc. 98 (2015) 1717–1723. doi:10.1111/jace.13526.

[97] A.L.G. Prette, M. Cologna, V. Sglavo, R. Raj, Flash-sintering of Co2MnO4 spinel for solid oxide fuel cell applications, J. Power Sources. 196 (2011) 2061–2065. doi:10.1016/j.jpowsour.2010.10.036.

[98] M. Biesuz, G. Dell'Agli, L. Spiridigliozzi, C. Ferone, V.M. Sglavo, Conventional and field-assisted sintering of nanosized Gd-doped ceria synthesized by co-precipitation, Ceram. Int. (2016) 1–6. doi:10.1016/j.ceramint.2016.04.097.

[99] R. Muccillo, E.N.S. Muccillo, M. Kleitz, Densification and enhancement of the grain boundary conductivity of gadolinium-doped barium cerate by ultra fast flash grain welding, J. Eur. Ceram. Soc. 32 (2012) 2311–2316. doi:10.1016/j.jeurceramsoc.2012.01.032.

[100] Y. Liu, X. Hao, Z. Wang, J. Wang, J. Qiao, Y. Yan, et al., A newly-developed effective direct current assisted sintering technique for electrolyte film densification of anode-supported solid oxide fuel cells, J. Power Sources. 215 (2012) 296–300. doi:10.1016/j.jpowsour.2012.05.017.

[101] J.S.C. Francis, M. Cologna, D. Montinaro, R. Raj, Flash sintering of anode-electrolyte multilayers for SOFC applications, J. Am. Ceram. Soc. 96 (2013) 1352–1354. doi:10.1111/jace.12330.

[102] C.E.J. Dancer, M. Achintha, C.J. Salter, J.A. Fernie, R.I. Todd, Residual stress distribution in a functionally graded alumina–silicon carbide material, Scr. Mater. 67 (2012) 281–284.

doi:10.1016/j.scriptamat.2012.05.002.

[103] C.E.J. Dancer, N.A. Yahya, T. Berndt, R.I. Todd, G. De Portu, Effect of residual compressive surface stress on severe wear of alumina-silicon carbide two-layered composites, Tribol. Int. 74 (2014) 87–92. doi:10.1016/j.triboint.2014.02.010.

[104] G. de Portu, L. Micele, Y. Sekiguchi, G. Pezzotti, Measurement of residual stress distributions in AlO/3Y-TZP multilayered composites by fluorescence and Raman microprobe piezo-spectroscopy, Acta Mater. 53 (2005) 1511–1520. doi:10.1016/j.actamat.2004.12.003.

[105] G. de Portu, L. Micele, G. Pezzotti, Laminated ceramic structures from oxide systems, Compos. Part B Eng. 37 (2006) 556–567. doi:10.1016/j.compositesb.2006.02.018.

[106] P.M. Vilarinho, A. Mahajan, I. Sterianou, I.M. Reaney, Layered composite thick films for dielectric applications, J. Eur. Ceram. Soc. 32 (2012) 4319–4326. doi:10.1016/j.jeurceramsoc.2012.05.026.

[107] S.-H. Yoon, M.-Y. Kim, C.-H. Nam, J.-W. Seo, S.-K. Wi, K.-H. Hur, Grain-growth effect on dielectric nonlinearity of BaTiO3-based multi-layer ceramic capacitors, Appl. Phys. Lett. 107 (2015) 072906. doi:10.1063/1.4929149.

[108] A. Karakuscu, M. Cologna, D. Yarotski, J. Won, J.S.C. Francis, R. Raj, et al., Defect Structure of Flash-Sintered Strontium Titanate, J. Am. Ceram. Soc. 95 (2012) 2531–2536. doi:10.1111/j.1551-2916.2012.05240.x.

[109] J.C. M'Peko, J.S.C. Francis, R. Raj, Field-assisted sintering of undoped BaTiO3: Microstructure evolution and dielectric permittivity, J. Eur. Ceram. Soc. 34 (2014) 3655–3660. doi:10.1016/j.jeurceramsoc.2014.04.041.

[110] A. Uehashi, H. Yoshida, T. Tokunaga, K. Sasaki, T. Yamamoto, Enhancement of sintering rates in BaTiO3 by controlling of DC electric current, J. Ceram. Soc. Japan. 123 (2015) 465–468. doi:10.2109/jcersj2.123.465.

[111] N. Shomrat, S. Baltianski, C.A. Randall, Y. Tsur, Flash sintering of potassium-niobate, J. Eur.

Ceram. Soc. 35 (2015) 2209–2213. doi:10.1016/j.jeurceramsoc.2015.01.017.

[112] T. Sun, X. Wang, H. Wang, X. Zhang, Z. Cheng, C.Q. Sun, et al., A phenomenological model on phase transitions in nanocrystalline barium titanate ceramic, J. Am. Ceram. Soc. 93 (2010) 2571–2573. doi:10.1111/j.1551-2916.2010.03900.x.

[113] G. Corapcioglu, M.A. Gulgun, K. Kisslinger, S. Sturm, S.K. Jha, R. Raj, Microstructure and microchemistry of flash sintered K0.5Na0.5NbO3, J. Ceram. Soc. Japan. 124 (2016) 321–328. doi:10.2109/jcersj2.15290.

[114] E. Castle, R. Sheridan, S. Grasso, A. Walton, M. Reece, Rapid Sintering of Anisotropic, Nanograined Nd-Fe-B by Flash-Spark Plasma Sintering, J. Magn. Magn. Mater. 417 (2016) 279–283. doi:10.1016/j.jmmm.2016.05.067.

[115] S.K. Jha, J.M. Lebrun, R. Raj, Phase transformation in the alumina–titania system during flash sintering experiments, J. Eur. Ceram. Soc. 36 (2016) 733–739. doi:http://dx.doi.org/10.1016/j.jeurceramsoc.2015.10.006.

[116] S.K. Jha, R. Raj, Electric Fields Obviate Constrained Sintering, J. Am. Ceram. Soc. 97 (2014) 3103–3109. doi:10.1111/jace.13136.

[117] R.K. BORDIA, R. RAJ, Sintering of TiO2-Al2O3 Composites: A Model Experimental Investigation, J. Am. Ceram. Soc. 71 (1988) 302–310. doi:10.1111/j.1151-2916.1988.tb05863.x.

[118] E. Bichaud, J.M. Chaix, C. Carry, M. Kleitz, M.C. Steil, Flash sintering incubation in Al2O3/TZP composites, J. Eur. Ceram. Soc. 35 (2015) 2587–2592. doi:10.1016/j.jeurceramsoc.2015.02.033.

[119] D. Liu, Y. Gao, J. Liu, K. Li, F. Liu, Y. Wang, et al., SiC whisker reinforced ZrO2 composites prepared by flash-sintering, J. Eur. Ceram. Soc. 36 (2016) 2051–2055. doi:10.1016/j.jeurceramsoc.2016.02.014.

[120] K.S. Naik, V.M. Sglavo, R. Raj, Field assisted sintering of ceramic constituted by alumina and

yttria stabilized zirconia, J. Eur. Ceram. Soc. 34 (2014) 2435–2442. doi:10.1016/j.jeurceramsoc.2014.02.042.

[121] Y. Waku, S. Sakata, A. Mitani, K. Shimizu, M. Hasebe, Temperature dependence of flexural strength and microstructure of Al2O3/Y3Al5 O12/ZrO2 ternary melt growth composites, J. Mater. Sci. 37 (2002) 2975–2982. doi:10.1023/A:1016073115264.

[122] D. Liu, Y. Gao, J. Liu, F. Liu, K. Li, H. Su, et al., Preparation of Al2O3–Y3Al5O12–ZrO2 eutectic ceramic by flash sintering, Scr. Mater. 114 (2016) 108–111. doi:10.1016/j.scriptamat.2015.12.002.

[123] K. Terauds, J.-M. Lebrun, H.-H. Lee, T.-Y. Jeon, S.-H. Lee, J.H. Je, et al., Electroluminescence and the measurement of temperature during Stage III of flash sintering experiments, J. Eur. Ceram. Soc. 35 (2015) 3195–3199. doi:10.1016/j.jeurceramsoc.2015.03.040.

[124] I.J. Hewitt, A.A. Lacey, R.I. Todd, A Mathematical Model for Flash Sintering, Math. Model. Nat. Phenom. 10 (2015) 77–89.

[125] Y. Dong, I.-W. Chen, Onset Criterion for Flash Sintering, J. Am. Ceram. Soc. 4 (2015) n/a–n/a. doi:10.1111/jace.13866.

[126] J.G.P. da Silva, H.A. Al-Qureshi, F. Keil, R. Janssen, A dynamic bifurcation criterion for thermal runaway during the flash sintering of ceramics, J. Eur. Ceram. Soc. 36 (2016) 1261–1267. doi:10.1016/j.jeurceramsoc.2015.11.048.

[127] J. Narayan, A new mechanism for field-assisted processing and flash sintering of materials, Scr. Mater. 69 (2013) 107–111. doi:10.1016/j.scriptamat.2013.02.020.

[128] J. Narayan, Grain growth model for electric field-assisted processing and flash sintering of materials, Scr. Mater. 68 (2013) 785–788. doi:10.1016/j.scriptamat.2013.01.008.

[129] R. Raj, Joule heating during flash-sintering, J. Eur. Ceram. Soc. 32 (2012) 2293–2301. doi:10.1016/j.jeurceramsoc.2012.02.030.

[130] K.S. Naik, V.M. Sglavo, R. Raj, Flash sintering as a nucleation phenomenon and a model thereof, J. Eur. Ceram. Soc. 34 (2014) 4063–4067. doi:10.1016/j.jeurceramsoc.2014.04.043.